SOURCES OF SALINIZATION OF THE BATON ROUGE AQUIFER SYSTEM:
SOUTHEASTERN LOUISIANA

A Thesis

Submitted to the Graduate Faculty of the
Louisiana State University and
Agricultural and Mechanical College
in partial fulfillment of the
requirements for the degree of
Master of Science

in

The Department of Geology and Geophysics

by
Callie Elizabeth Anderson
B.S., Louisiana State University, 2010
May 2012

ACKNOWLEDGEMENTS

The M.S. Thesis Committee for this project included Prof. Jeffrey Hanor (Chair), Department of Geology and Geophysics, Prof. Frank Tsai from the Department of Civil Engineering, and Prof. Carol Wicks from the Department of Geology and Geophysics. I appreciate each of their support and guidance. Sincerest thanks to Dr. Hanor for spending countless hours working with and teaching me and for his patience and unwavering support.

Finally, I thank my mother, Beth, for the constant encouragement, guidance, and for pushing me to be my best through my entire academic career.

TABLE OF CONTENTS

LIST OF FIGURES

ABSTRACT

A major environmental and economic problem confronting the Baton Rouge area, southeastern Louisiana, is the progressive salinization of the Baton Rouge aquifer system, an important source of fresh municipal and industrial groundwater. The Baton Rouge fault marks a boundary between fresh groundwaters to the north and predominately brackish waters to the south. Determining the permeability architecture of the fault is an essential component of modeling groundwater flow and saline contamination north of the fault. Understanding the sources and pathways of the saline waters that are migrating into the freshwater sands north of the fault is thus essential in helping to establish fault permeability.

This study has confirmed that plumes of saline water extend vertically upward above the top of salt at the St. Gabriel field south of Baton Rouge, a suspected source of saline water. The plumes may have been produced by the episodic expulsion of waters from overpressured sediments at depth. Spatial variations in formation water salinity support the conclusion that there has been lateral migration of shallow saline waters northward from the St. Gabriel field toward the Baton Rouge fault. There is a shallow plume of saline water which has migrated to the northwest in the lower part of the Mississippi River Alluvial Aquifer, and a more diffuse brackish zone below this where there has been mixing of saline waters from St. Gabriel with fresh meteoric waters from the Baton Rouge aquifer sands to the north. There are also well-defined tongues of fresh water that have moved laterally across the fault to the south. The results of the present research support the conclusion that there has been extensive lateral migration of waters across the Baton Rouge fault in the past rather than vertical migration up the fault. Although the presumed anisotropy in permeability of the fault zone should favor flow vertically

up the fault over flow perpendicular to the fault, the large density contrast between the fresh and

brackish waters above a depth of 3,000 feet with the highly saline waters below may inhibit this.

INTRODUCTION

A major environmental and economic problem faces the Baton Rouge, Louisiana metropolitan area. The Baton Rouge aquifer system, the main source of both industrial and residential water use for the city, has been undergoing salinization (Long, 1965; Lovelace, 2007; Tsai, 2010). The aquifer system is made up of twelve freshwater sandy units, most of which have experienced some degree of salinization in the last fifty years (Lovelace, 2007; Tsai and Li, 2008). Ten of these aquifers are named after their depths in the Baton Rouge industrial area. These freshwater sandy units are the "400-foot", the "600-foot", the "800-foot", the "1,000-foot", the "1,200-foot", the "1,500-foot", the "1,700-foot", the "2,000-foot", the "2,400-foot", and the "2,800-foot" sands (Lovelace, 2007). The saltwater intrusion issues are the result of increased pumping in the Baton Rouge area, which causes changes in the hydraulic gradient (Rollo, 1969). The Baton Rouge freshwater aquifers were initially separated from brackish water sands to the south by the Baton Rouge fault, which has apparently acted as a leaky hydraulic barrier. However, with the change in hydraulic gradient, brackish water from the south and/or from depth is making its way across or up the fault northward into the freshwater sands.

One of the biggest questions regarding the hydrology of the area is the role of the Baton Rouge fault as either a barrier and/or a conduit to fluid flow (Bense and Person, 2006) and whether that flow occurs in a vertical fashion up the fault zone or occurs laterally across the fault. Such information is a critical component in efforts to develop groundwater flow and solute transport models for the area. Stoessell and Prochaska (2005) suggested, based on Sr isotope ratios and other chemical data, that the saline waters travel vertically up fault planes from depth. A study by Bense and Person (2006) cited the Baton Rouge fault as an example of vertical fluid movement through fault zones. That study also suggested that in some places along the fault

vertical transport may be occurring due to high hydraulic head gradients up the fault. A 2004-2005 study of chloride concentrations in the groundwater (Lovelace, 2007) showed that the highest chloride concentrations in aquifer sands occur at mid-depth in the aquifer system rather than at the base. Wendeborn and Hanor (2008) concluded that vertical transport up the fault was unlikely as the main pathway of the saltwater flow, because in addition to that fact that the highest chloride concentrations in the freshwater sands occur at mid-depths in the Baton Rouge aquifer system instead of the base, as would be expected with vertical transport. There was also noticeable lateral interfingering of fresh and brackish water across the fault. Wendeborn and Hanor (2008) therefore concluded that the more likely source of the saline waters is salt domes to the south of Baton Rouge (Figure 1.1), with lateral transport across the fault.

Rollo (1969) calculated the rates at which the salt-water fronts will reach the industrial pumping centers in the 600 ft, 800 ft, 1000 ft, 1200 ft, 1500 ft, and 2000 ft sands. Rollo's calculations gave a range of 10-80 years for these aquifers. A much more recent study was done by Tsai and Li (2008) of saltwater intrusion in the Baton Rouge aquifer system and they developed a regional model for saltwater intrusion using the program SEAWAT to better understand the movement of salt water. The groundwater flow simulations showed strong lateral movement of saline waters across the Baton Rouge fault toward a cone of depression in the areas of heavy pumping (Figure 1.2). This study is a good example of why understanding the pathways of saline water movement is essential. The Tsai and Li model showed that by year 2080 salinities of 100 ppm could reach the Baton Rouge pumping centers at Lula Avenue (Figure 1.2) face the very serious threat of saltwater intrusion. This in turn would have serious consequences on residential and industrial use of the aquifer. In the scenario where lateral transport is hypothesized to occur across the fault, as in the Tsai and Li (2008) study, for the salt source
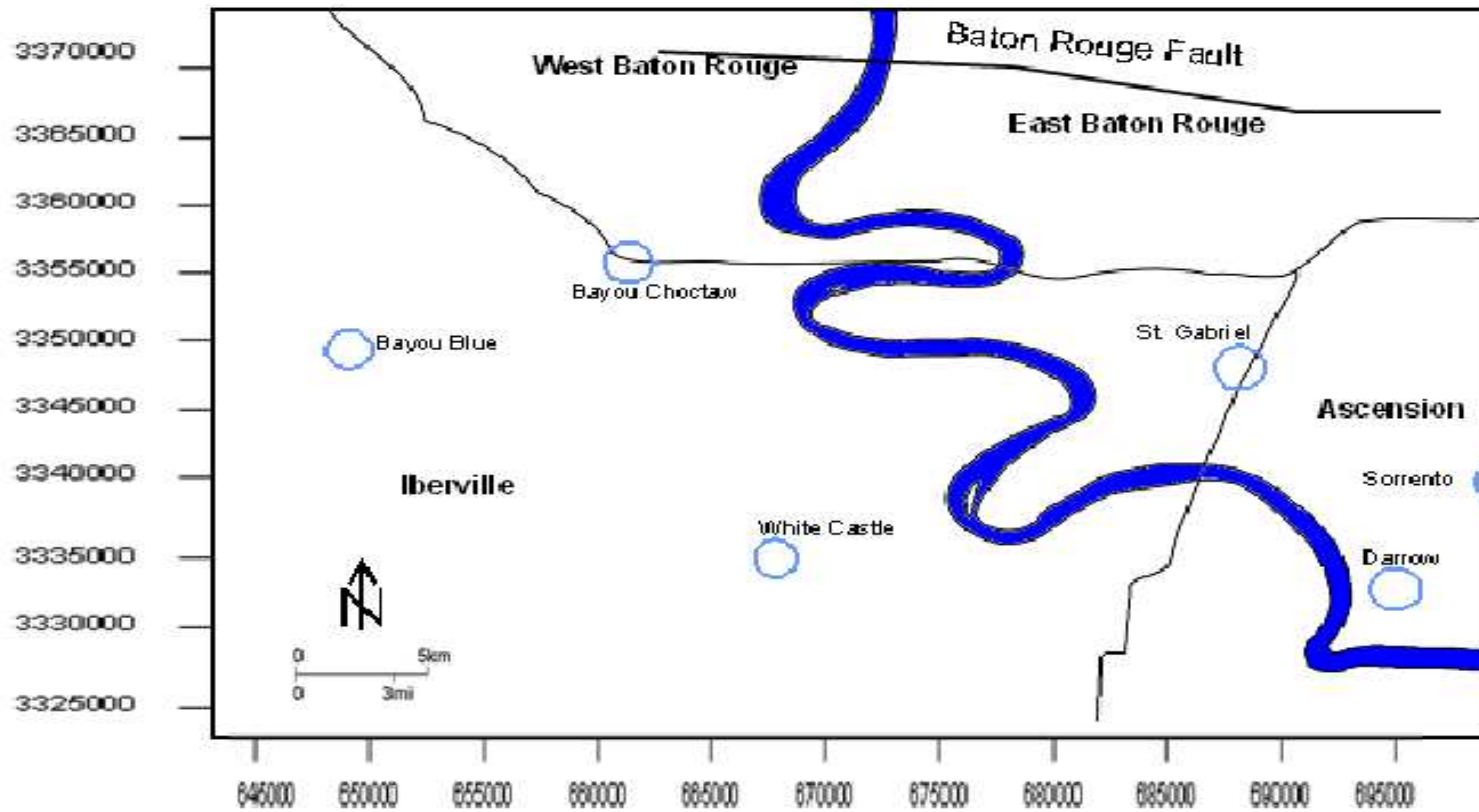
Figure 1.1. A map of study area showing location of the Baton Rouge fault, Mississippi River, parish boundaries, and locations of salt domes south of Baton Rouge. (modified from Bray and Hanor, 1990) Location coordinates are given in UTM.
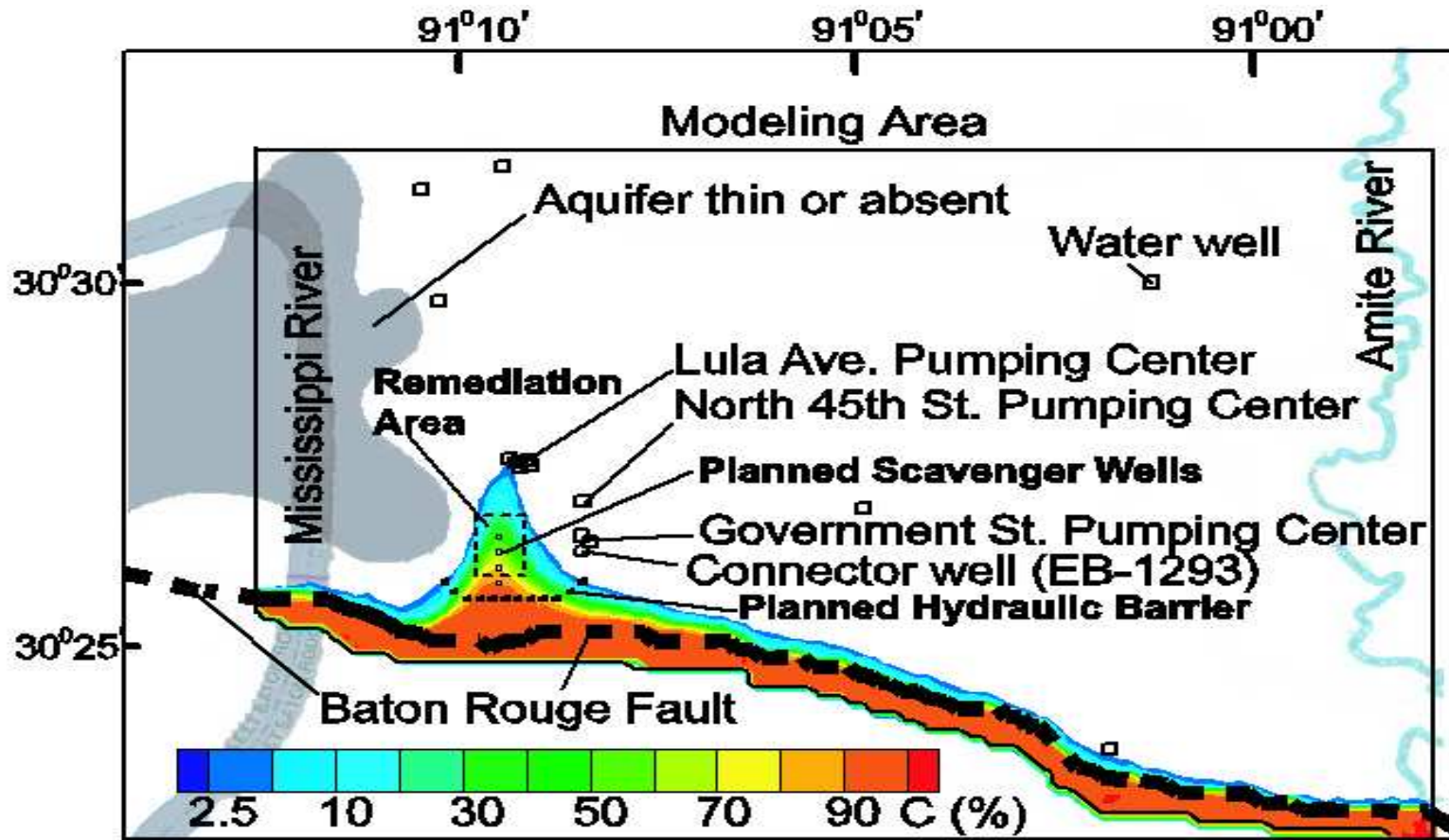
Figure 1.2. A map by Tsai (2010) of the Baton Rouge area showing migration of salty water to the north across the Baton Rouge fault and toward the Lula Avenue pumping center in the 1,500 foot sand of the Baton Rouge aquifer at the beginning of 2005. C (%) expresses the concentration of end-member saltwater present.

would more likely be located to the south of Baton Rouge. Wendeborn and Hanor (2008) suggested one possible salt source is the St. Gabriel salt dome, which is one of the main sources of the elevated salinity present in sediments directly south of Baton Rouge (Bray and Hanor, 1990). In this hypothesis, the saline waters travel vertically up faults associated with the dome, and into shallower sands. Eventually the saline waters would migrate laterally into the freshwater zone north of the Baton Rouge fault. A groundwater study by Long (1965) showed the absence of fresh water above the St. Gabriel salt dome (Figure 1.3). A regional cross section by Bray and Hanor (1990) (Figure 1.4) showing spatial variations in groundwater salinity through the Baton Rouge area to the St. Gabriel and Darrow domes to the south shows plumes of high salinity near the edges of the dome. In addition, the cross section indicates that no fresh water is present in the immediate vicinity of the dome.

One goal of this research was to test the hypothesis that the St. Gabriel area is a source of the saline waters presently contaminating the Baton Rouge aquifer system, and that there has been predominantly lateral flow of saline waters across the Baton Rouge fault as opposed to vertical flow up the fault. A second hypothesis was that spatial variations in salinity can be used to determine sources and pathways of migration of saline waters. The research had two components. The first was to determine if there has been migration of saline waters upward from the St. Gabriel salt dome into shallow sediments, and the second was to determine if there has been northward migration of saline waters from St. Gabriel into the Baton Rouge area, explained in detail in the Methods and Results chapters. This research is part of a long-term program designed to investigate the role of salt dissolution on the local and regional hydrogeology of the northern Gulf of Mexico sedimentary basin (e.g. Hanor, 1984; Hanor and Sassen, 1990; and Hanor and Mercer, 2010).
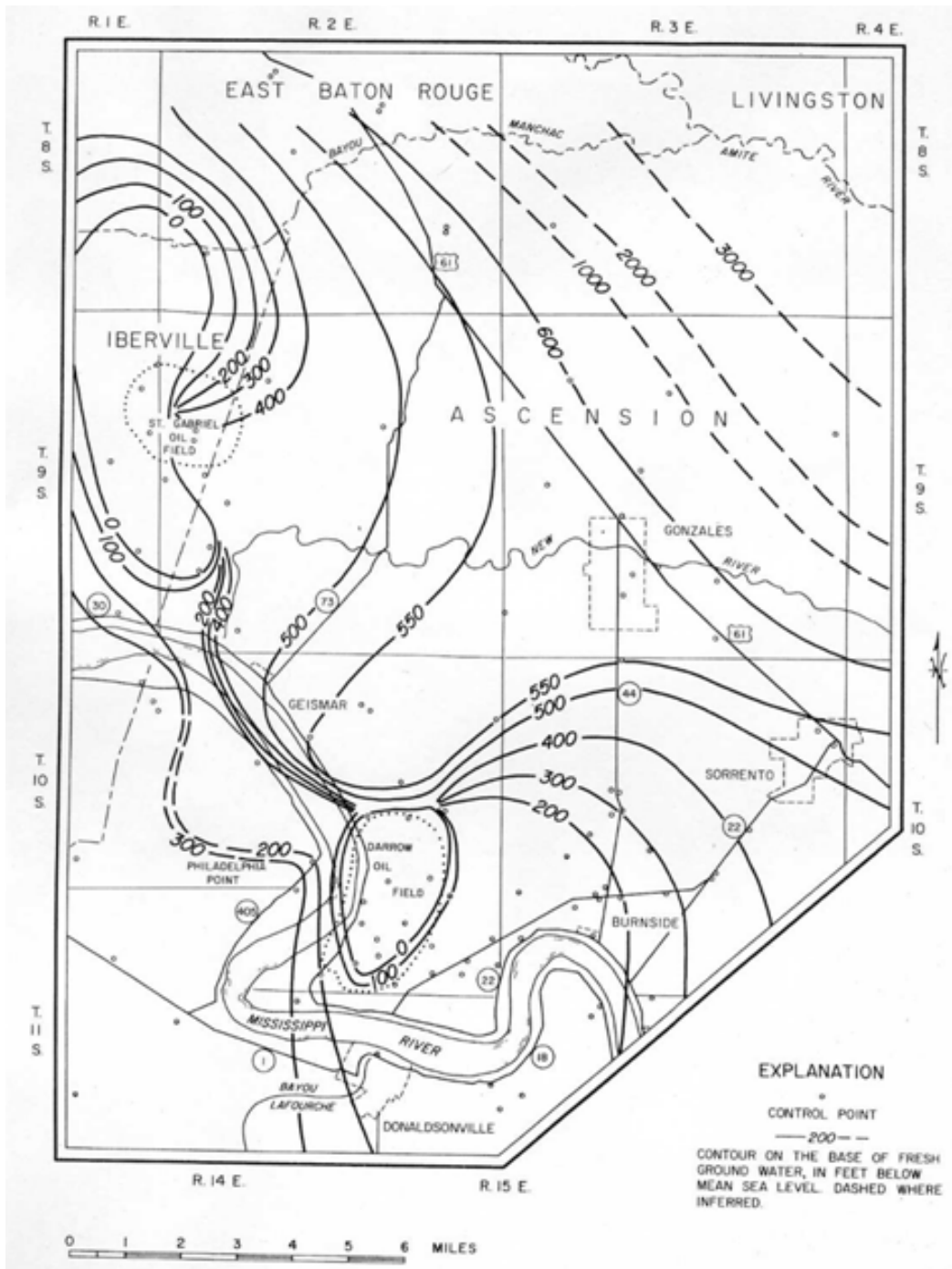
Figure 1.3. A map showing the depth to the base of fresh groundwater in Iberville and Ascension parishes from Long (1965). Note the lack of fresh groundwater above the St. Gabriel salt dome in the northwest corner of the map.
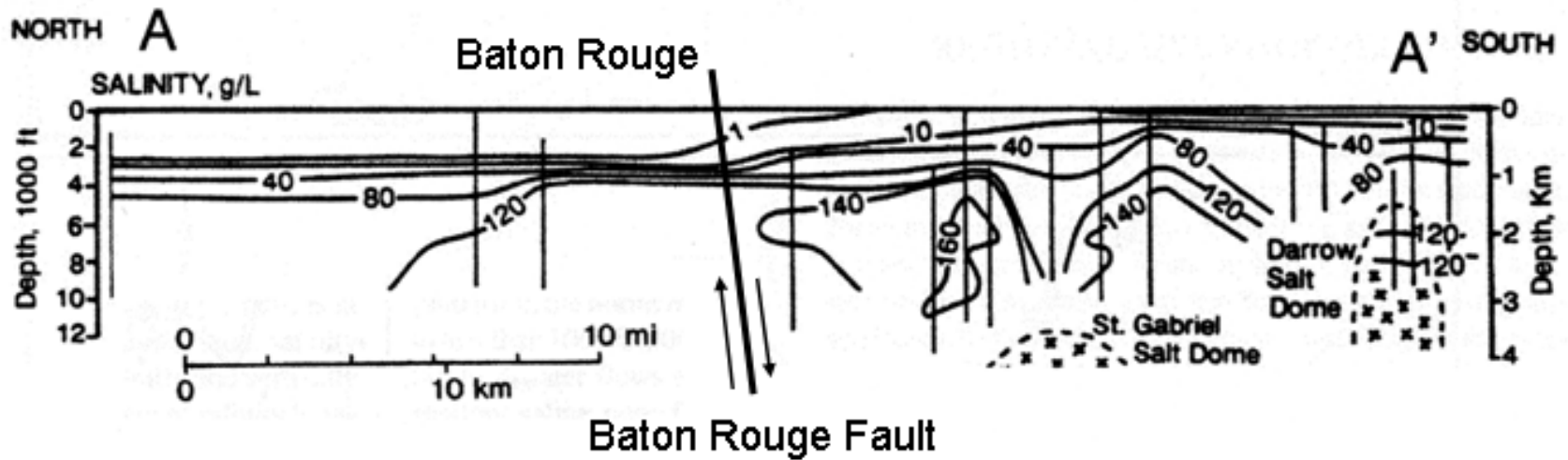
Figure 1.4. A north-south cross section showing the variations in groundwater salinity across the Baton Rouge area and the St. Gabriel and Darrow salt domes (modified from Bray and Hanor, 1990). For reference the salinity of seawater is 35 g/L. Note salinity plumes above the St. Gabriel salt dome.

GEOLOGIC SETTING

The St. Gabriel Field

One area which has been identified as a possible source for the saltwater intrusion is the St. Gabriel salt dome, located approximately 9 miles (15 kilometers) south of Baton Rouge, near the boundary between Ascension and Iberville parishes (Figure 1.1). The sediments overlying salt date from the Eocene to Recent alluvial deposits (Holyoak, 1965). Sands overlying the structure are interbedded with shales, limy shales, and thin limestones. Top of salt at the St. Gabriel dome is approximately 11,000 feet (4 kilometers) in depth (Holyoak, 1965). The St. Gabriel field is a known hydrocarbon producer of dominantly oil and condensate, but also produces gas (Holyoak, 1965). The exact geometry of the structure is not known, but overlying sequences and the top of salt are shown in a cross section by NOGS (1965) (Figure 2.1). Normal faults associated with the dome and structure of surrounding sediments could be conduits for vertical fluid transport, and possibly lateral transport in some areas (Figure 2.2). There are three major fault systems associated with the dome, down to the northeast, down to the northwest, and down to the south (Holyoak, 1965).

The Baton Rouge Aquifer System

The Baton Rouge aquifer system consists of a 2,800 ft (850 m) thick sequence of complexly interbedded fluvial sands and mudstones occurring in the metropolitan Baton Rouge area, southeastern Louisiana. The fresh water aquifer sediments here range in age from the late Miocene to the Pleistocene and dip to the south (Lovelace, 2007) (Figure 2.3). This local aquifer system is part of two regional aquifer systems designated by the U.S.G.S.: the Coastal Lowlands aquifer system, which, according to the usage of Martin and Whiteman (1989) includes

8
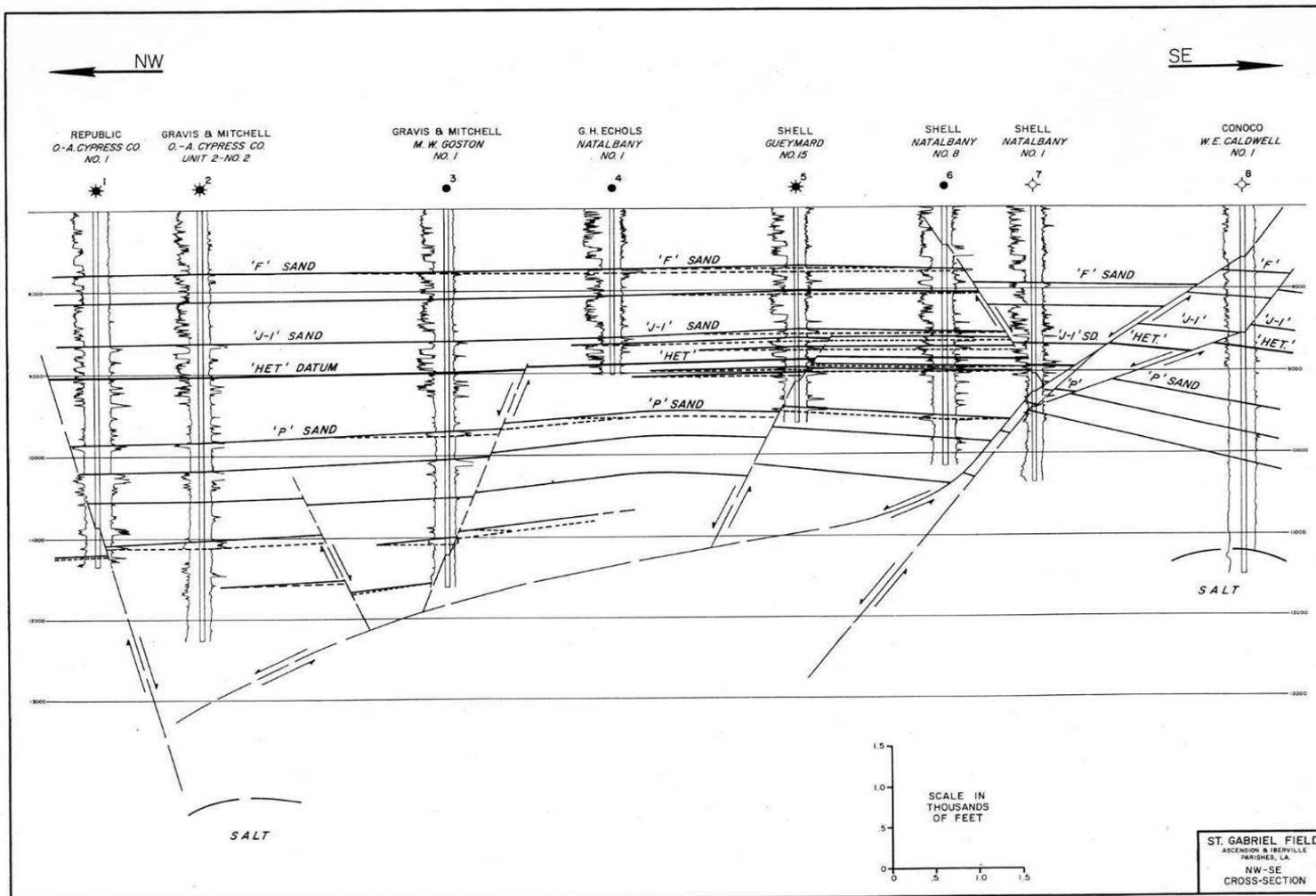
Figure 2.1. A cross section of the St. Gabriel field from Holyoak (1965) showing stratigraphy and structure of sand units overlying the St. Gabriel salt dome. Faults associated with the dome are also visible. Two areas where wells have pierced the salt as of the year 1965 are shown at depths of 11,230 and 14,290 feet (3,400 and 2,350 m).
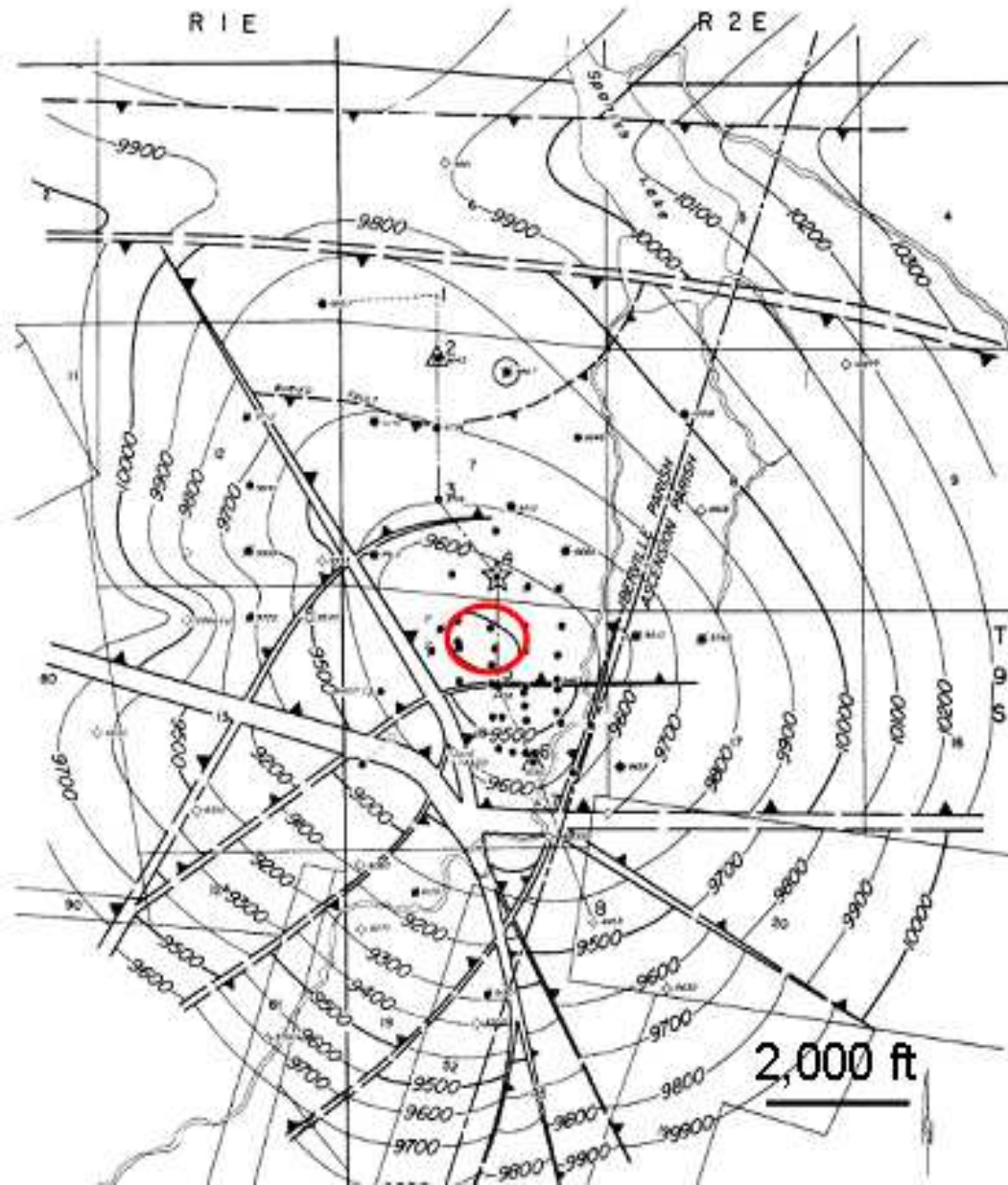
Figure 2.2. A structure map of the top of the P sand, which overlies the St. Gabriel salt dome, and associated faults (NOGS, 1965). The red circle indicates the location of the shallowest depth to the P sand (Figure 2.1). Shallowest salt known as of 1965 lies at borehole 8 in the map, south of the crest of the structure.

Figure 2.3. Dipping sandy layers of the Baton Rouge aquifer system (Griffith, 2008). Light green-blue areas represent freshwater aquifers, and pink represents brackish/saline aquifers. Note the locations of the Baton Rouge fault and of the St. Gabriel field.

sediments in Louisiana, Mississippi, Alabama, and Florida, and the Southern Hills or Chicot Equivalent aquifer system, which includes aquifer units only in southeastern Louisiana and southwestern Mississippi. The Southern Hills aquifers are recharged primarily north of the Louisiana-Mississippi border over a wide area of southwestern Mississippi, and regional flow is to the south (Rollo, 1969). Pre-developmental discharge areas for the aquifers are located as far inland as 60 miles (100 kilometers) from the Gulf of Mexico (Hanor et al., 2007). The Southern Hills sediments generally thicken down dip, and transition into thick deltaic and marine sequences offshore (McFarlan and LeRoy, 1988). At the time of their deposition, these sediments contained fresh to normal marine water. However, some now contain waters with salinities several times that of seawater (Bray and Hanor, 1990). Three distinct regional fluid flow regimes exist in south Louisiana, a shallow fresh water regime, which includes the Southern Hills aquifer, that is topographically driven, a deep overpressured fluid regime, and an intermediate depth interval of hypersaline waters that are driven by density differences caused by spatial variations in temperature and salinity (Hanor and Sassen, 1990). It has been shown that (e.g., Bennett and Hanor, 1987) that the variations in salinity within this zone are the result of the subsurface dissolution of salt domes and subsequent solute transport.

The salt from which the south Louisiana salt domes were formed is the Louann salt evaporites. The breakup of Pangea and the associated rifting in what is now the Gulf of Mexico region began in the Triassic and continued into the Jurassic. There was intrusion of seawater into the newly created Gulf, and the deposition of a regional evaporite unit as much as a kilometer or more in thickness in the Middle Jurassic (Salvador, 1991). Salt deformation processes have been active since the time of the deposition of the Louann, forming domes and other salt structures in many areas of south Louisiana (Salvador, 1991).

The Mississippi River Alluvial Aquifer

Later Pleistocene sands, which range from 300-900 feet thick (90-270 meters) also include the Mississippi River Alluvial Aquifer (MRAA), which is Pleistocene alluvial materials of Early Illinoian through Late Wisconsinian age (McFarlan and LeRoy, 1988) that were deposited unconformably over older Pleistocene sediments, and cut by the present Mississippi River (Whiteman, 1972) (Figs 2.4, 2.5). The changing course of the Mississippi River during the deposition of the MRAA caused reworking and sorting, leaving large braided stream deposits of mostly sand and gravel, with varying thicknesses exceeding 400 feet (120 meters) (Figure 2.6) (Whiteman, 1972).

The Baton Rouge Fault

The Baton Rouge fault is a west-east trending, south-dipping listric fault in Louisiana, which offsets a thick sequence of unconsolidated siliciclastic sediments, including the sediments which make up the Baton Rouge aquifer system (Figure 2.3). The Baton Rouge fault is a reactivated Cenozoic fault, which was first active in the late Eocene/Early Oligocene and remained active until the late Oligocene (McCulloh and Heinrich, 2012). The fault was reactivated in the Pleistocene, and the older aquifer sands in the Baton Rouge area are offset by the same slip, between 300-350 feet (91-107 meters) (McCulloh and Heinrich, 2012). The fault is of significant hydrogeologic and environmental importance because it marks a fairly sharp boundary between fresh water sands to the north and brackish water sands to the south.
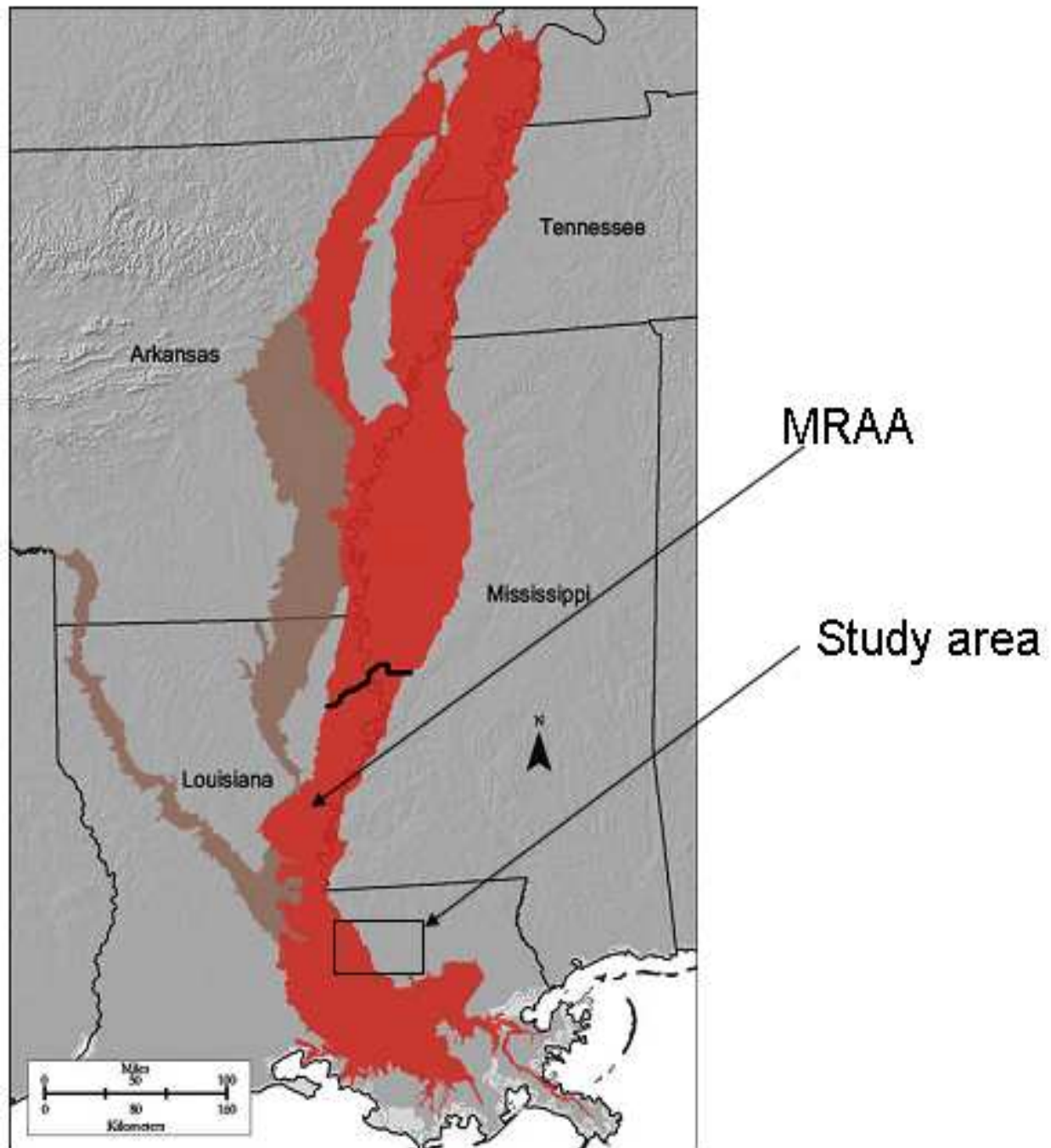
Figure 2.4. A map showing the location of the Mississippi River Alluvial Aquifer (MRAA), shown in red (modified from Welch and Hanor, 2011). The study area is outlined with the box, illustrating the section of the study area where the MRAA is present.
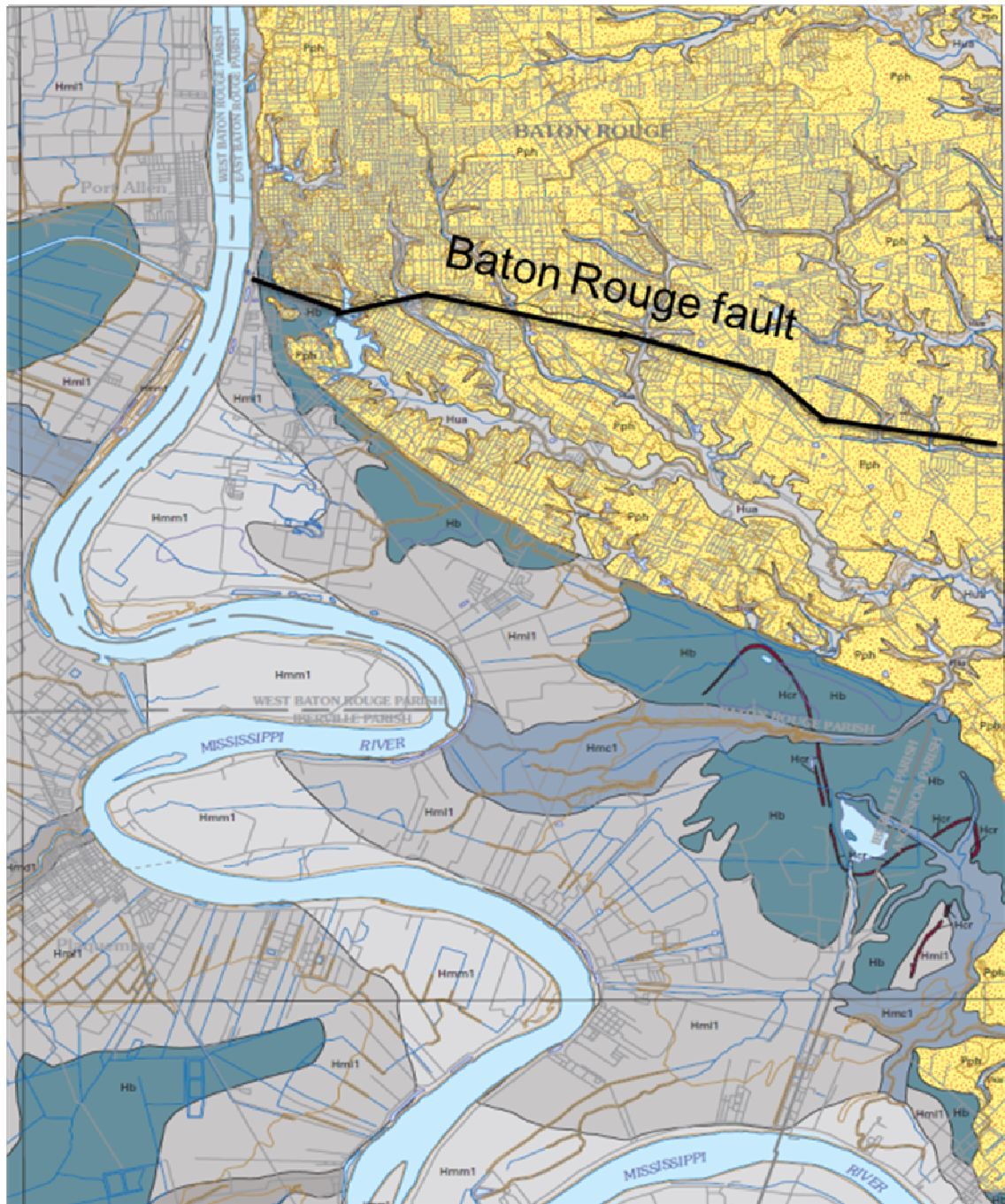
Figure 2.5. A geologic map showing the Baton Rouge quadrangle (modified from Heinrich and Autin, 2000). The tan-brown color represents sediment that overlie the Mississippi River Alluvial Aquifer, and the yellow color represents sediment that overlies the Baton Rouge aquifer system.
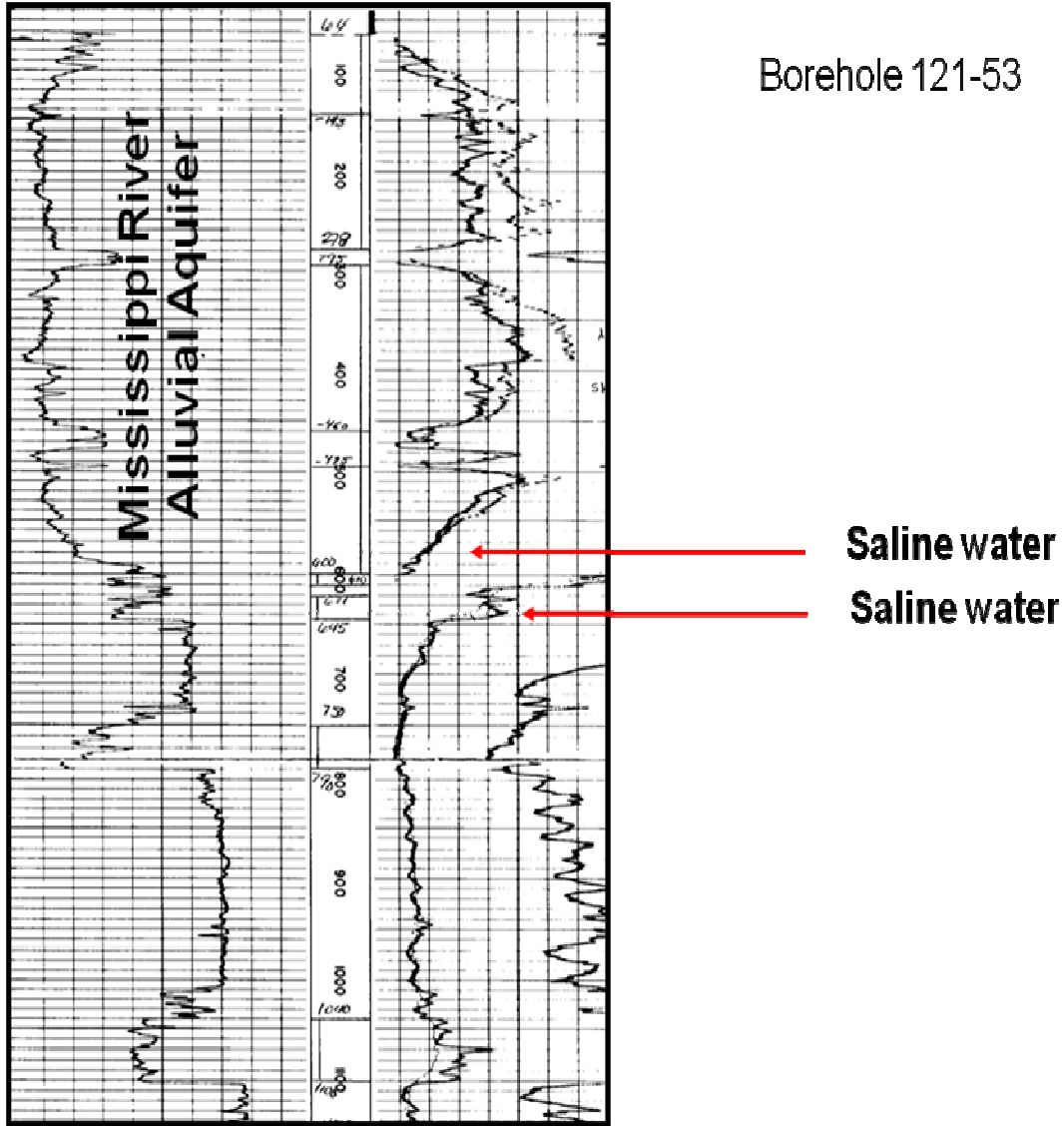
Figure 2.6. A spontaneous potential reading from well 121-53 (Appendix I), illustrating the thick sands of the Mississippi River Alluvial Aquifer (MRAA). High resistivities throughout most of the log indicate the presence of relatively freshwater. The drop in resistivity near the bottom of the unit indicates a change to brackish water. Note low resistivity (high salinity) in sands directly under the MRAA (750-800 ft), where saline water has leaked down into older Pleistocene sands.

METHODS

Introduction

Much of the data used in this study were generated from wireline spontaneous potential (SP) and resistivity logs made in the course of oil and gas exploration and production and for development of groundwater supplies. A total of 69 logs were used in the St. Gabriel field study, with the majority made in the 1960s. Data on salinity and temperature derived from 46 of these were from an earlier unpublished study by Hanor (personal communication, 2011), two logs from the Long (1965) study were used, and 21 were selected from the collections of the Louisiana Geological Survey (LGS). An additional 39 logs were utilized in the regional study at and north of St. Gabriel. Of these, 19 were log images provided by Dr. Frank Tsai (LSU Department of Civil and Environmental Engineering). It was necessary to download the headers for these logs from the Louisiana Department of Natural Resources SONRIS site so that salinity calculations from SP response could be made. Data from an additional 19 logs were obtained from a previous study done by Wendeborn and Hanor (2008). Locations and logging dates for these boreholes are given in Appendix I.

 Calculating Salinity from Spontaneous Potential

Salinities and temperatures had previously been calculated for St. Gabriel field using data from spontaneous potential (SP) and resistivity logs in an unpublished study by J.S. Hanor (Hanor, personal communication, 2011). Salinities in this previous study were calculated from charts in Schlumberger and similar log interpretation books (Gearhart-Owen, 1974).

Salinities were calculated for the area immediately south of the Baton Rouge fault to the St. Gabriel salt dome at a shallow depth interval between 500 and 3,000 feet (150-910 m) using SP and resistivity logs. Salinities were calculated from SP using an Excel spreadsheet program

developed by Hanor (personal communication) for calculating formation water salinities and Rw from SP response using an algorithm by Bateman and Konen (1977). Input values for the spreadsheet were taken from the well header information and measured directly from the SP log reading, including the depth of the log reading, the mud weight, the uncorrected bore hole temperature for top and bottom of a logging run, the resistivity of the fluid at a recorded temperature, the resistivity of the mud filtrate at a certain temperature, and the SSP reading. In addition, the Wendeborn and Hanor study (2008) generated salinity calculations from wells directly north and south of the Baton Rouge fault.

For log headers missing mud weights, an average of 10 lbs/gallon was assumed because this is the average mud weight from other wells used in this study. Many of the older logs were also missing data for the resistivity of the mud filtrate, Rmf. These missing values were calculated from the measured resistivity of the mud at the measured temperature, and corrected to a temperature of 75°C using the relationship between resistivity and resistivity of mud filtrate from the Hilchie (1984) equation: $R_m(75) = R_m(T_m) * ((T_m+6.77)/(75+6.77))$. Using the R_m calculated for 75°C, the resistivity of the mud filtrate can be calculated using the equation: $0.64*10^{-2} + 0.81172*R_{mud}$. This relation was derived based on a linear comparison of the known mud filtrate values from other wells used in this study.

Calculating Salinity from Resistivity

Salinities from resistivity were calculated by first calculating a formation factor for the aquifer. The Archie equation was used with Humble constants (a, m) for clean sands, $F = a/\phi^m$, where F is the formation factor, ϕ is porosity, a = 0.62, and m = 2.15. For the purposes of this study, porosity was assumed to be 0.4, based on average porosity for medium-coarse grained sand. Water resistivity (Rw) can then be calculated using the relationship Rw=Ro/F, where

18

sediment resistivity (Ro) is measured from the resistivity log in units of ohm-m. Groundwater

electrical conductivity (Cw) is the reciprocal of Rw, and has units of S/m. Salinity (TDS) can

then be calculated using the equation: TDS = 0.5778*Cw+7.1069 (Welch and Hanor, 2011),

where TDS is expressed in parts per million (ppm).

Temperature and Temperature Gradients

Bottom hole temperatures (BHTs) were acquired from well headers. Ground surface

temperature was assumed to be 75°F. Missing bottom hole temperatures for SP calculations were

estimated by graphing the trends of bore hole temperature versus depth for the other wells in the

study area. Bottom hole temperatures were corrected using the equation $BHT_{corrected} = BHT_{measured}$

$+ (33 - (0.265*(z/1,000) - 11.7)^2)$, where z is depth in feet (Funayama and Hanor, 1990). The true

temperature gradient is the first derivative of temperature with respect to elevation (dT/dz).

Apparent temperature gradients are the temperature change over a larger interval, such as from

depth to the surface (Figure 3.1). Apparent temperature gradient was calculated using the

equation: apparent $T_{gradient}$= (corrected bottom hole T - surface T)/ (depth interval). These

apparent temperature gradient calculations were done for wells over St. Gabriel salt dome and

were used as an input variable in density calculations in a regional cross section through the

study area.

***In Situ* Fluid Density**

In situ fluid densities were calculated using two separate algorithms. For salinities greater

than that of seawater (35,000 ppm), the Phillips et al. (1983) algorithm for NaCl solutions was

used. However, it is known that this algorithm yields erroneously high densities for waters less

saline than seawater (Funayama and Hanor, 1990). For groundwater salinities less than that of

seawater, the algorithm by Stuyfzand (1993), which was developed for mixed fresh
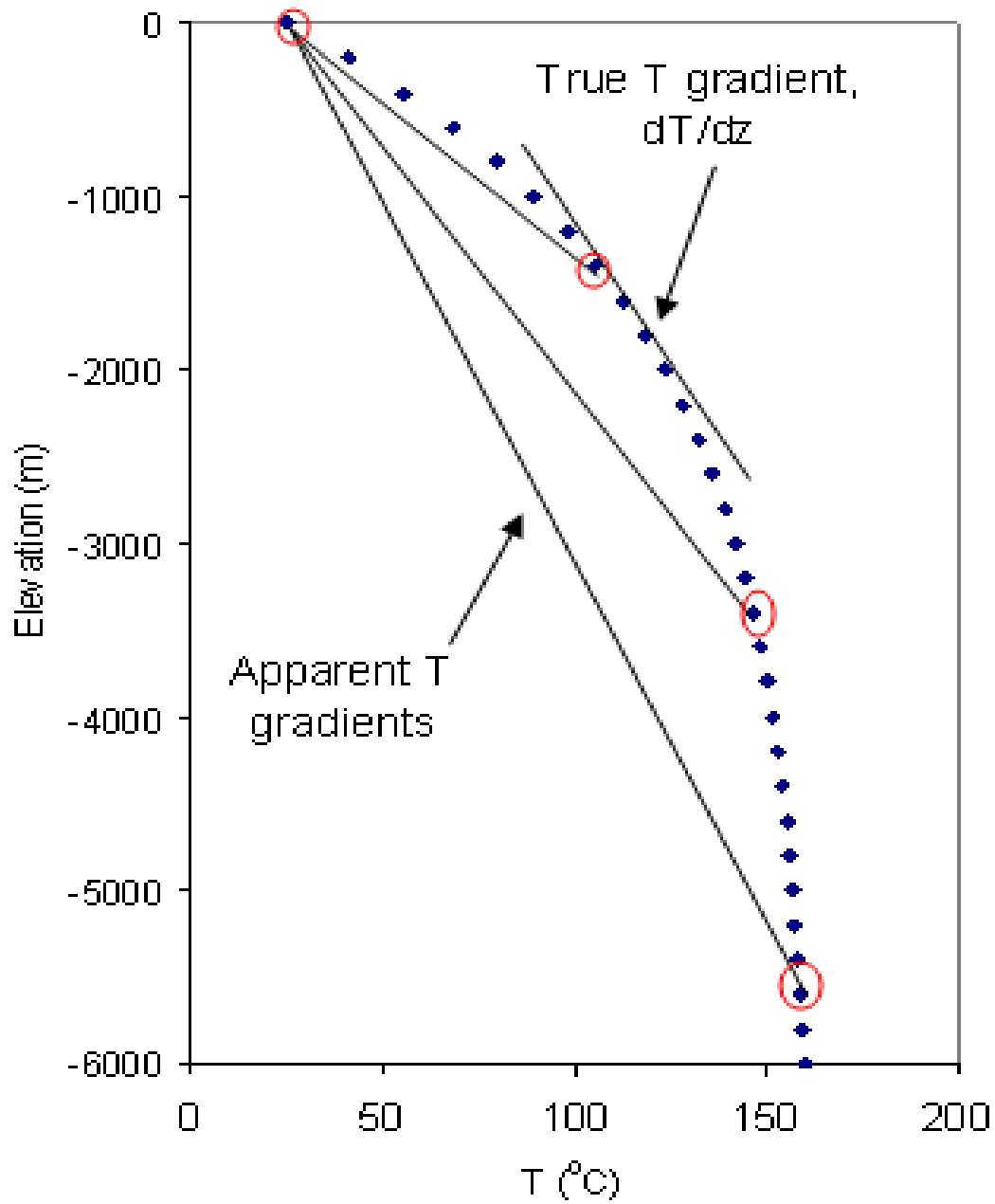
Figure 3.1. A graph showing change of temperature with depth at a hypothetical site, and illustrating the concepts of true temperature gradients and apparent temperature gradients.

groundwaters and seawater, is more accurate. Input variables for these calculations included

calculated salinities, temperature gradient, and depth. Depth was used as a proxy to calculate

pressure, using the relation: $z * g * 1,000 = P$, where z is depth in meters, g is the gravitational

constant (9.81 m/s^2), and P is pressure. This equation gives pressure in units of Pascals, which

was then converted to bars and used in density calculations.

Solute and Heat Transport Calculations

Salinity plumes above salt at St. Gabriel were first noted in Bray and Hanor (1990) and

were also documented in this study (Results chapter). To understand mechanisms responsible for

salinity plumes around the St. Gabriel salt dome, vertical transport equations were explored.

Simple, one-dimensional, steady-state groundwater solute and heat transport equations were used

to estimate possible rates of hypothetical vertical fluid flow. An equation by Bredehoft and

Papadopulos (1965) was used for temperature variations as a function of depth for hypothetical

one-dimensional, steady-state conditions:

$T(z) = T(u) + (T(L) * f(\beta, z/L)$,

where $\beta = (c_w \rho_w q_w L)/K_m$

C_w= heat capacity of fluid (J/kg-K)
ρ_w= density of fluid (kg/m^3)
q_w= Darcy velocity (m/s)
L= distance (m)
K_m=thermal conductivity of medium (J/m * s * K)

Values used for the calculations in this study can be found in Appendix II.

An analogous equation by Finlayson (1992) was used to calculate solute concentration as

a function of depth for hypothetical one-dimensional, steady-state conditions:

$C(z) = C(U) + (C(L)-C(U) * f(\xi, z/L))$,

where $\xi = (q_w L)/ \phi D$ and $D=((\alpha_L q_w)/ \phi) + D_m$

21

q_w= Darcy velocity (m/s)
L= Distance (m)
ϕ= porosity (m^3/m^3)
D= diffusion-dispersion coefficient (m^2/s)
α_L= longitudinal dispersivity (m)
D_m= sediment diffusion coefficient (m^2/s)

Values used for calculations in this study can be found in Appendix II.

Spatial Variations in Salinity and *In Situ* Fluid Density

The salinity data were used to create horizontal slice maps for the St. Gabriel field from 500 to 1,000 foot intervals between 500 and 9,000 feet for salinity. The slice maps were created in Golden Software Surfer 7.0. These data were also used to create a cross-section of salinity variations from the northwest to the southeast across the St. Gabriel field area. Salinity contour maps were also created for the regional study area, using Golden Software Surfer 10.0. Starting at 500 feet in depth, maps were created at 500 foot (150 m) intervals to a depth of 3,000 feet (910 m). Three cross sections were made for salinity across the regional study area, at a depth interval between 500-4,000 feet (150-1,200 m). One cross section was created showing in situ fluid density from just north of the fault to the edge of the St. Gabriel field area, for a depth interval of 500 to 4,000 feet (150-1,200 m).

RESULTS

The St. Gabriel Field

Salinity

Horizontal salinity contour maps were created at a depth of 500 feet (150 m) then 1,000 foot (300 m) intervals starting at a depth of 1,000 feet (300 m) to show the spatial variations of salinity at the St. Gabriel field area (Figure 4.1, A-J). The contour maps made for depths shallower than 3,000 feet (<910 m), used borehole logs from both the unpublished Hanor study and the LGS (Figure 4.1, A-C). The red circle on each of the maps indicates the location of the top of structure.

At a depth of 500 feet (150 m), while well control is very sparse, it is clear that no fresh water is present (Figure 4.1, A). Salinities range between 5 and 12.5 g/L, which is less than the salt content of seawater but still brackish. Well control is still sparse at a depth of 1,000 feet (300 m), but does show that waters at this shallow depth have elevated salinities, but are less than seawater salinity (35 g/L) for most of the study area. An area of much higher salinity (90 g/L) is present in the southwestern corner of the study area at a depth of 1,000 feet (Figure 4.1, B). At a depth of 2,000-foot (610 m) there are areas of high salinity both to the north and south of the top of the dome (Figure 4.1, C).

Salinity contour maps at depths greater than 3,000 ft (>910 m) and deeper were created using logs from the unpublished Hanor study. The slice maps from 3,000- 7,000 ft (910-2100 m) show a strong general trend of high salinity areas around the margins of the dome, with a relative low over the top of the structure (Figure 4.1, D-H). The two deepest maps, at 8,000 and
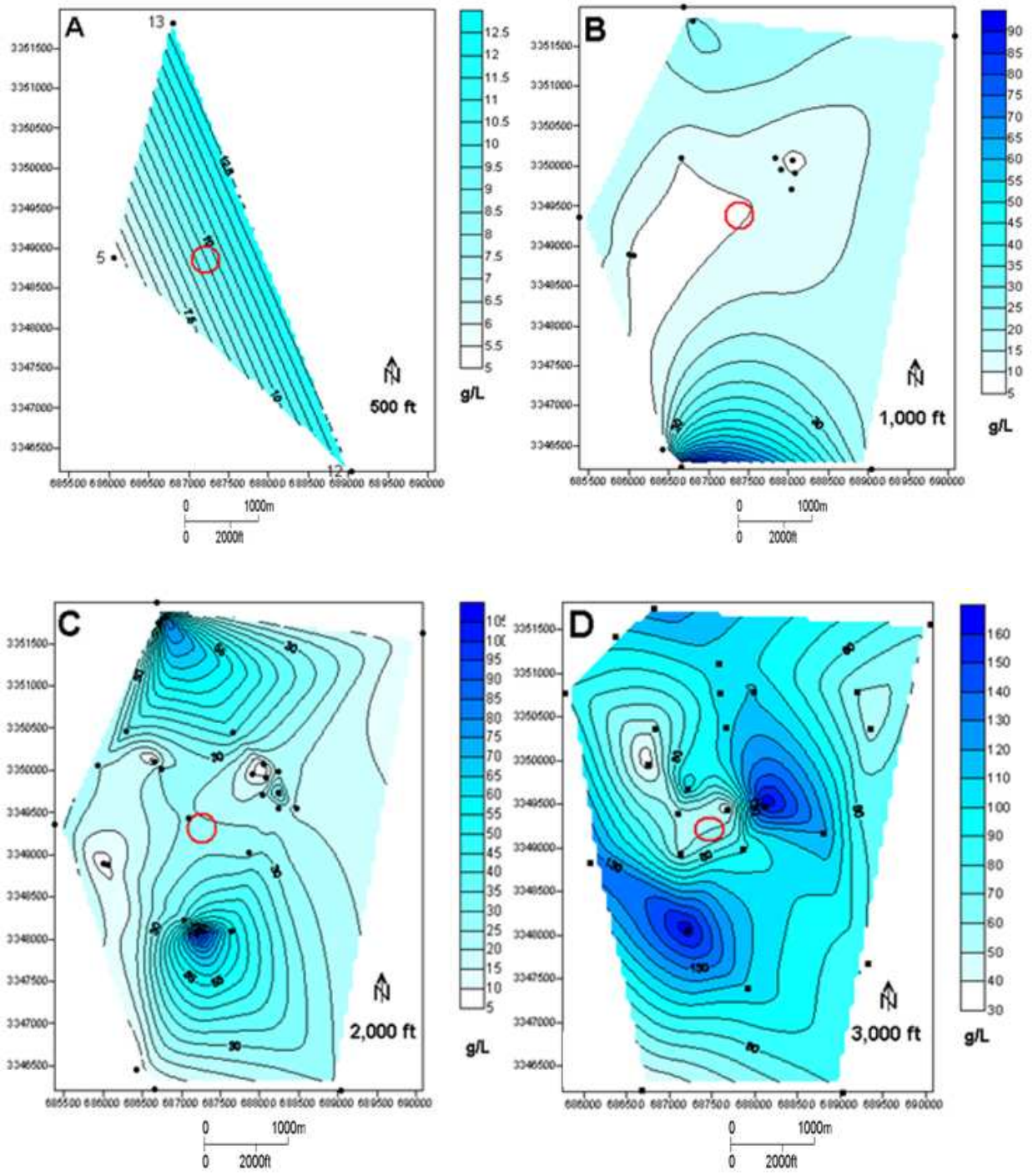
Figure 4.1. Spatial variations in salinity from the St. Gabriel field at varying depths below land surface. The red circle represents the top of the domal structure (Figure 2.2). Location grid is given in UTM coordinates.

24

(Figure 4.1 continued)
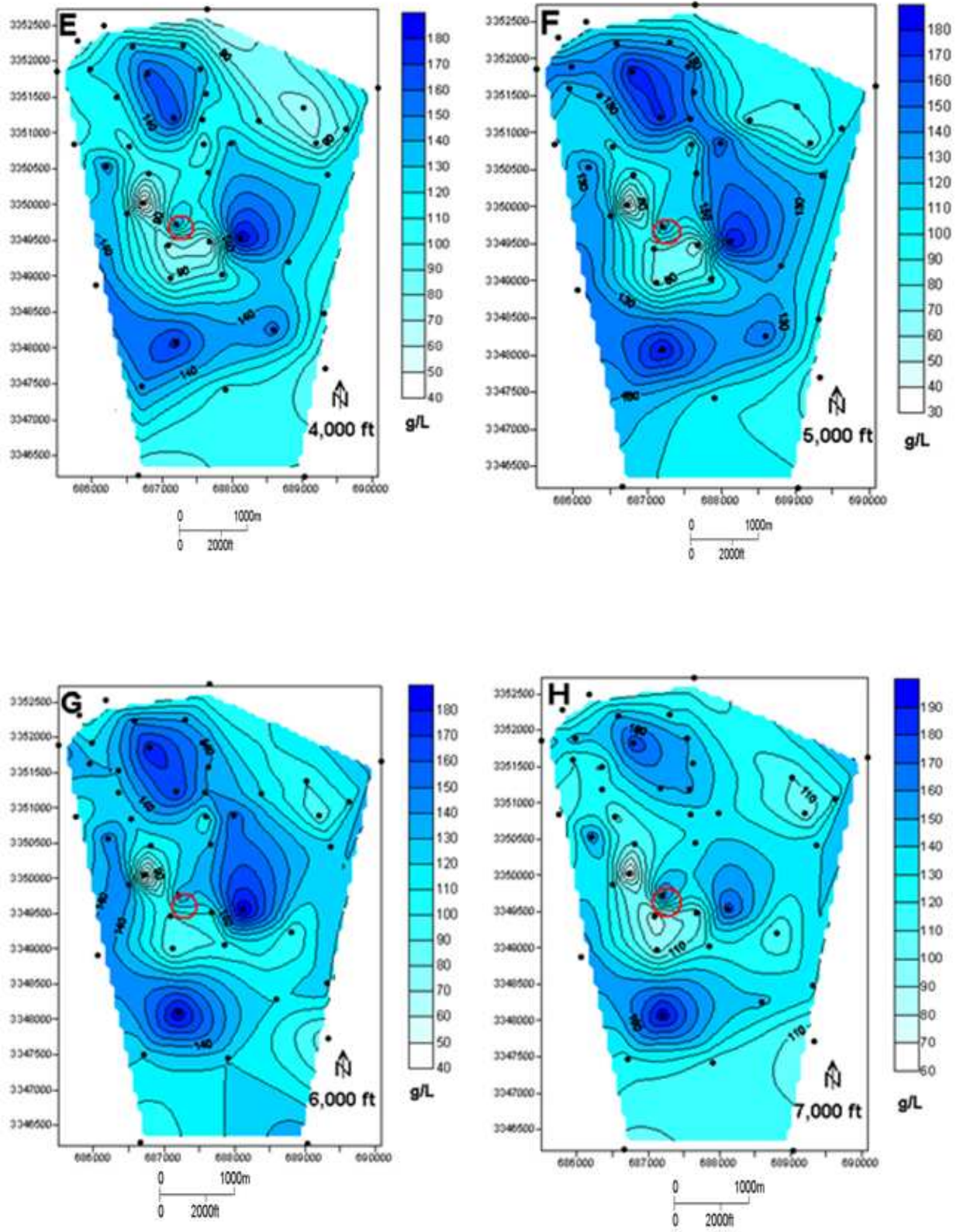
(Figure 4.1 continued)
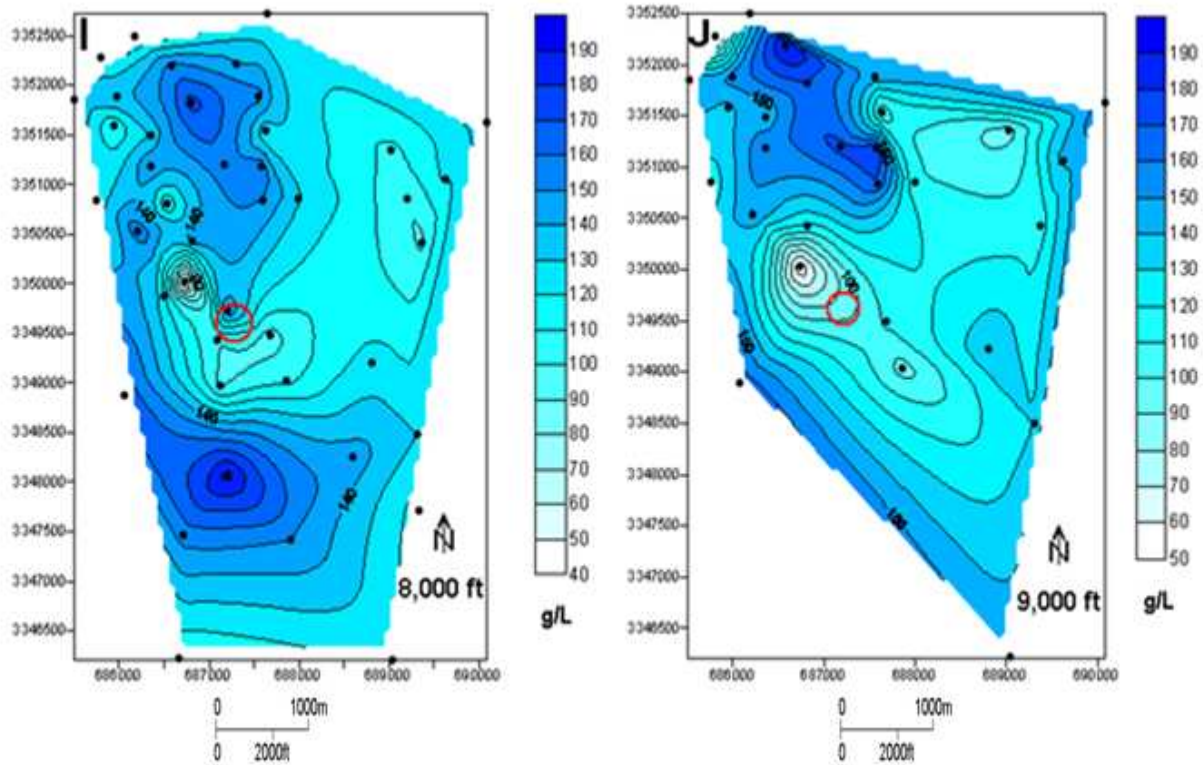
9,000 ft (2400-2700 m) show some differences from the shallower levels, particularly the disappearance of one major high salinity plume to the east of the top of the dome structure (Figure 4.1, I-J). Well control becomes sparser at these greater depths. The general spatial pattern is that of higher salinities being located in an annular area around the shallowest part of the structure above salt with a relative salinity low above the top of the structure.

A salinity cross section was created through the St. Gabriel field area from the northwest to the southeast (Figure 4.2). This cross section highlights the significant differences between the salinities around the margins and over the top of the structure and shows the location of salinity plumes extending upward from salt.

Temperature and Temperature Gradients

Apparent temperature gradients range from 18-35 °C/km across the field (Figure 4.3). Like the spatial variations in salinity, there is a general trend of higher temperature gradients occurring around the margin of the domal structure, with relative lows above the top of the structure. The high temperature gradient areas generally correspond spatially with the salinity plumes, particularly at depths of 3,000-7,000 ft (910-2100 m) (Figure 4.1, C-G). However, the correlation is not perfect, and an area of high temperature gradient that does not correspond with a high salinity plume is present on the northeast corner of the area (Figure 4.3). An overlay of the areas of high salinity with the areas of high apparent temperature gradients illustrates that although both occur in an annular pattern around the apparent top of structure, there is not a perfect match (Figure 4.4). In addition, when plotted as a function of depth, there were several data points for apparent temperature gradient that were unrealistically high for shallow depths, between 40-60 °C/km for a depth of 1,000 ft (300 m) (Figure 4.5). One data point shows 120°C/km at a depth less than 1,000 feet (<300 m), but this data point is thought to be an error (Figure 4.5).

Heat and Solute Transport Modeling

The spatial variations in formation water salinity documented in this study suggest the existence of plumes of saline waters having been expelled vertically upward through the sedimentary sequence overlying salt. Because the driving mechanisms for this possible fluid expulsion have not yet been identified, no attempt was made try to develop a rigorous solute transport model for the field. However, it is possible to make some very approximate estimates of what fluid velocities might be involved if it is assumed, as described in the Methods section, that solute transport is steady-state and one-dimensional.
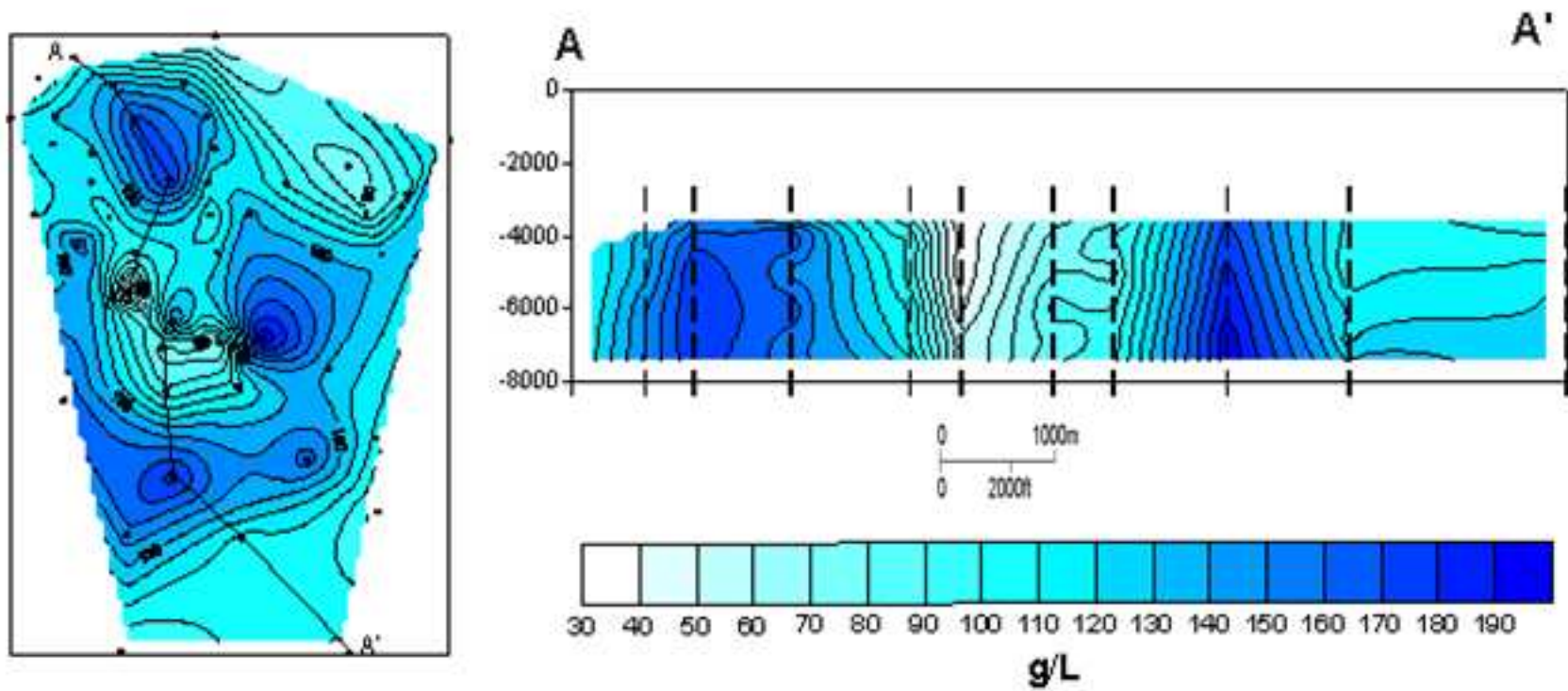
Figure 4.2. A location map at a depth of 4,000 ft and cross section showing spatial variations in salinity from the St. Gabriel field. Top of control is at approximately 3,000 ft.
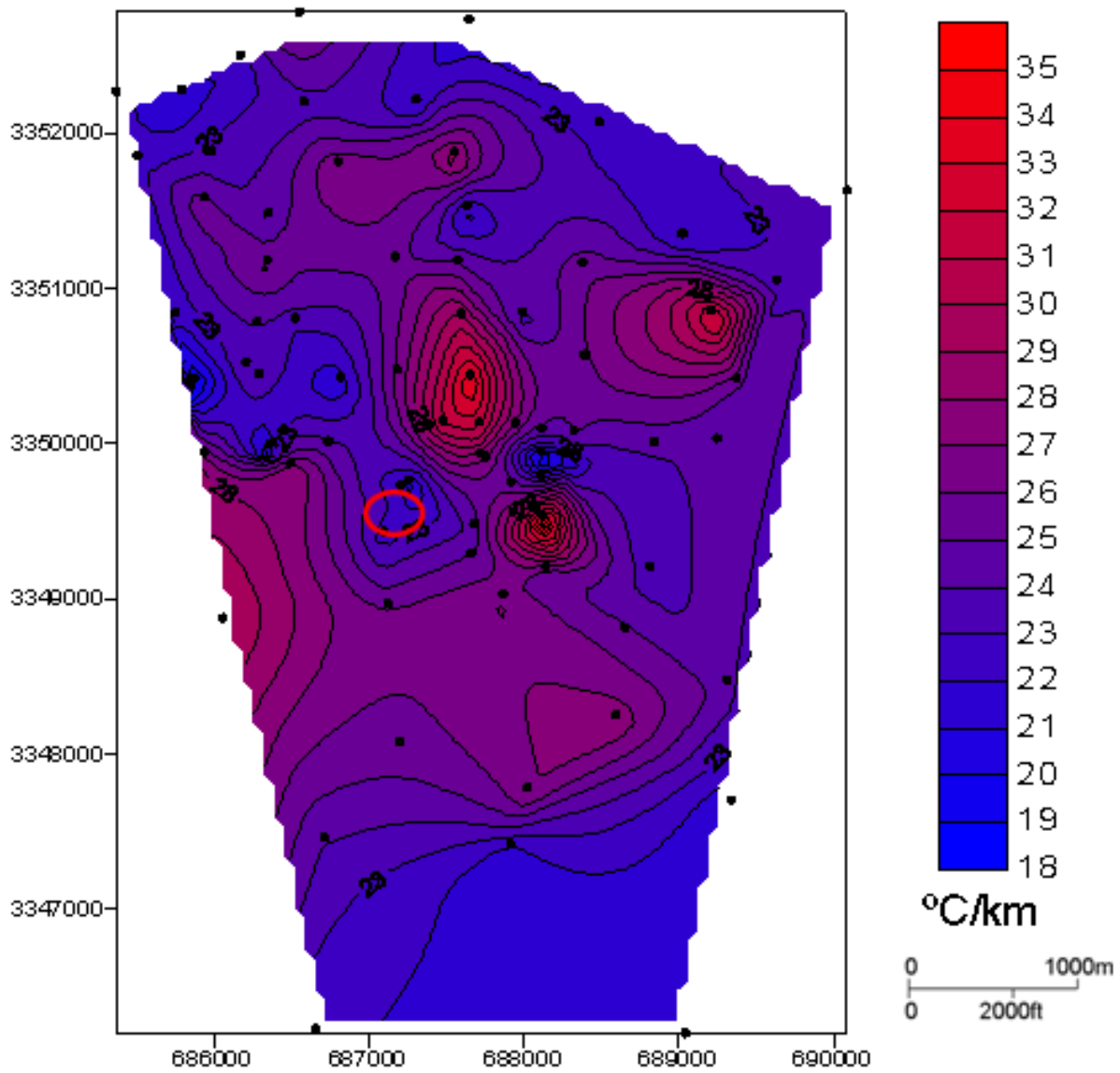
Figure 4.3. A contour map showing spatial variations in apparent temperature gradients at the St. Gabriel field. The red circle represents the top of structure. Location grid is given in UTM coordinates.
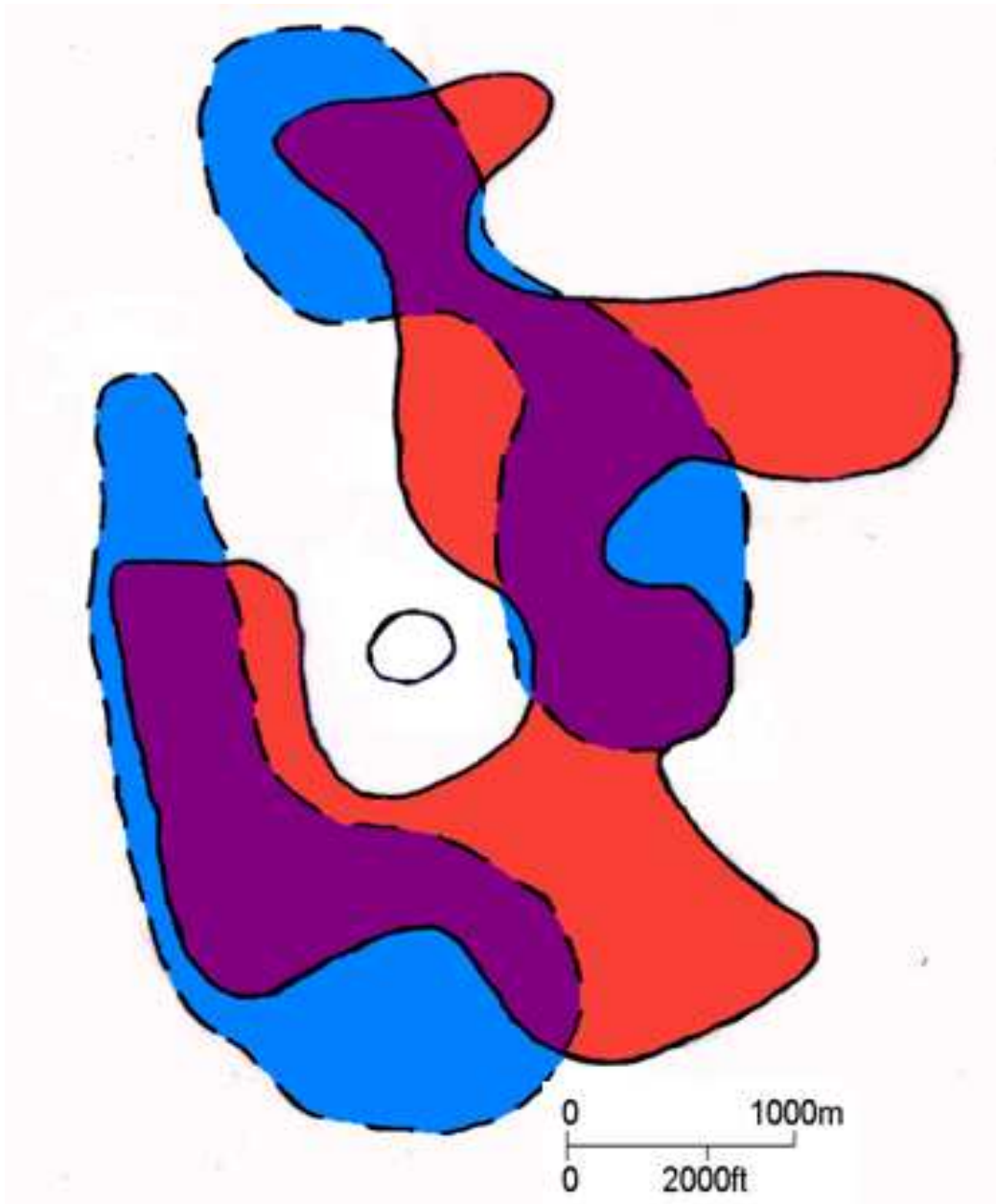
Figure 4.4. A graph illustrating similarities in spatial variations of salinity and apparent temperature gradients over the St. Gabriel field. Red areas show the areas of high apparent temperature gradient, from Figure 4.3. Blue areas show areas of high salinity, at a depth of 6,000 feet (Figure 4.1, G). Purple indicates an area of high salinity and apparent temperature gradient. The circle in the middle represents the top of structure.
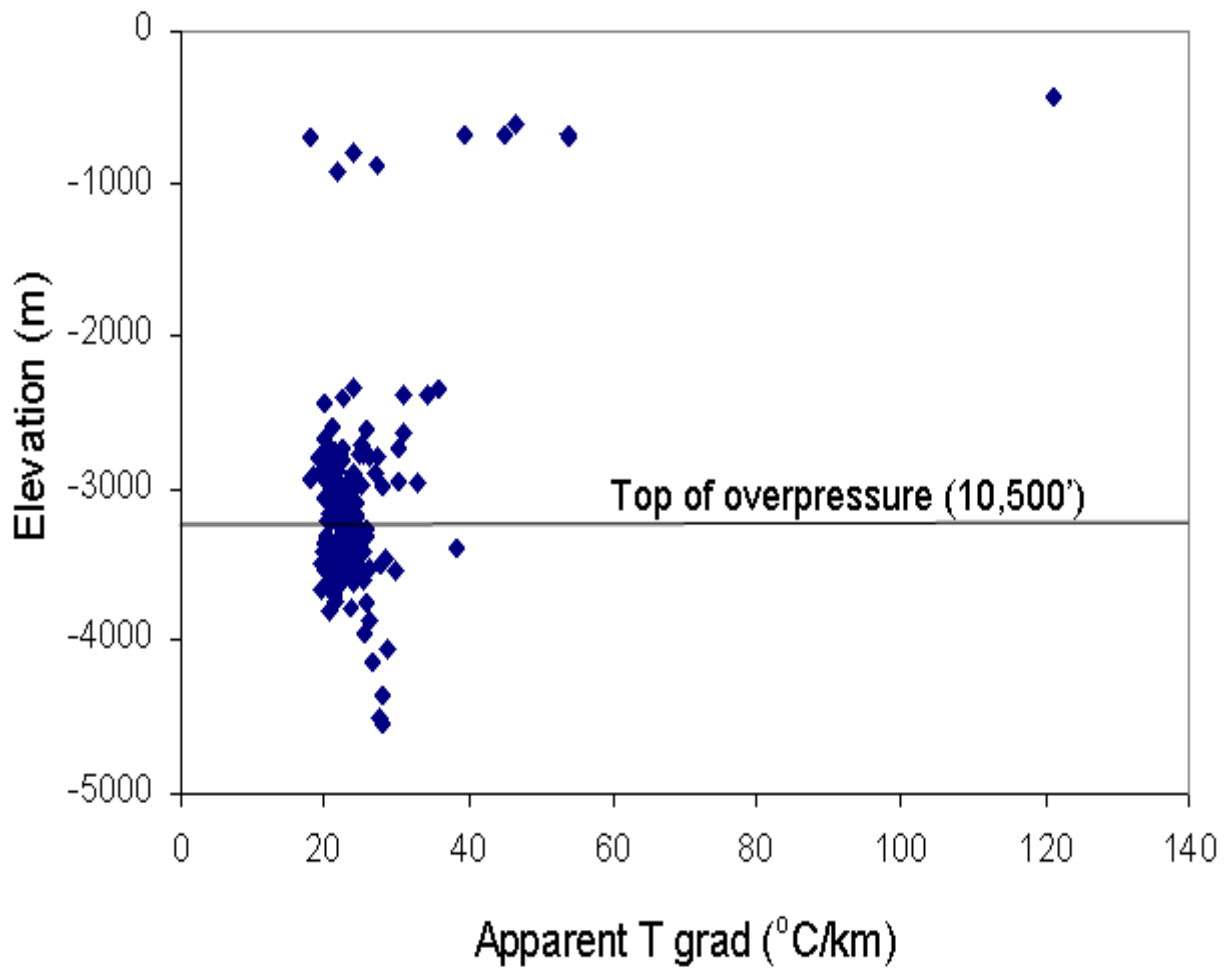
Figure 4.5. A graph showing apparent temperature gradients from the St. Gabriel field as a function of depth or elevation. High apparent temperature gradients at shallow depths may represent a non-linear increase in temperature with depth, which could reflect upward advective transport of heat.

It was found through a sensitivity analysis that the temperature profiles generated using the Bredehoft and Papadopulos equation are very sensitive to fluid velocities. A true fluid velocity of 2.4 cm/y gives a reasonable fit to the corrected bottom hole temperatures at the St. Gabriel field (Figure 4.6). The model temperatures (Figure 4.7 A) yield high true gradients and apparent gradients at shallow depths, and lower gradients at deeper depths. The profile reflects dominance by advective heat transport at depth with an increase in the importance of conductive transport at shallow depths. The same fluid velocities tested in the heat transport modeling were used in the solute transport modeling using the equation of Finlayson (Figure 4.7 B). At a velocity of 2.4 cm/y, solute transport is dominated by advection over almost the entire vertical column, and there is a negligible decrease in salinity upward. Diffusive transport becomes important only very near the ground surface, and there is in an abrupt decrease in salinity at very shallow depths.

Regional Study

Salinity

Salinity contour maps were created for the regional study area at 500 ft (150 m) depth intervals between 500 and 3,000 ft (150-910 m). The regional study area extends from the St. Gabriel salt dome to just north of the Baton Rouge fault (Figure 4.8). A plume of salty water extends from the St. Gabriel field to the northeast at depths of 500 and 1,000 ft (150 and 300 m) (Figure 4.9 A-B). This area of high salinity occurs generally within the Mississippi Alluvial Aquifer, and appears to cross the Baton Rouge fault to the east of the Mississippi River. In addition to presence of saline waters north of the fault, freshwater exists south of the fault at various depths. Relatively fresh water occurs over a large area of West Baton Rouge Parish at a depth of 500 ft (150 m) to the west of the river (Figure 4.9 A). Fresh water also exists in a
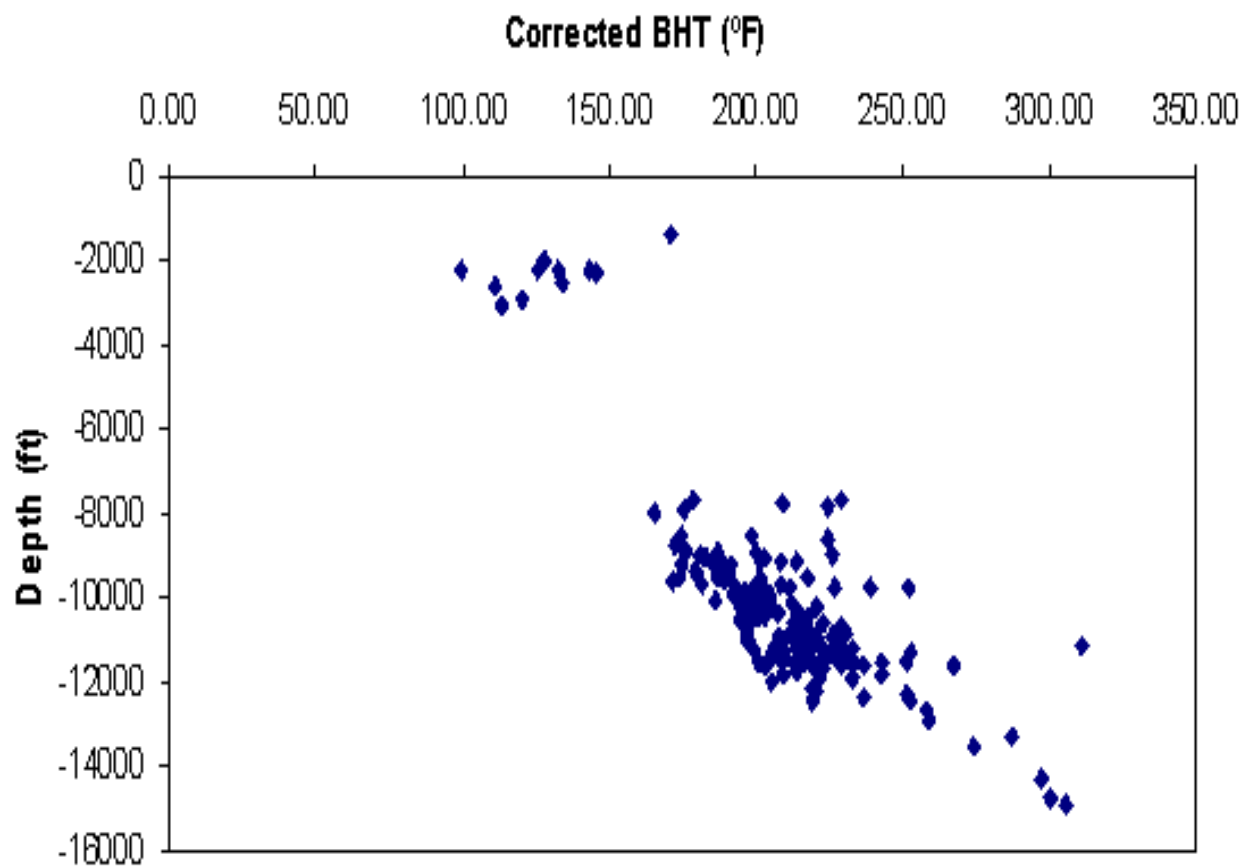
Figure 4.6. Corrected bottom hole temperature (in °F) with depth (in feet) from the St. Gabriel field.
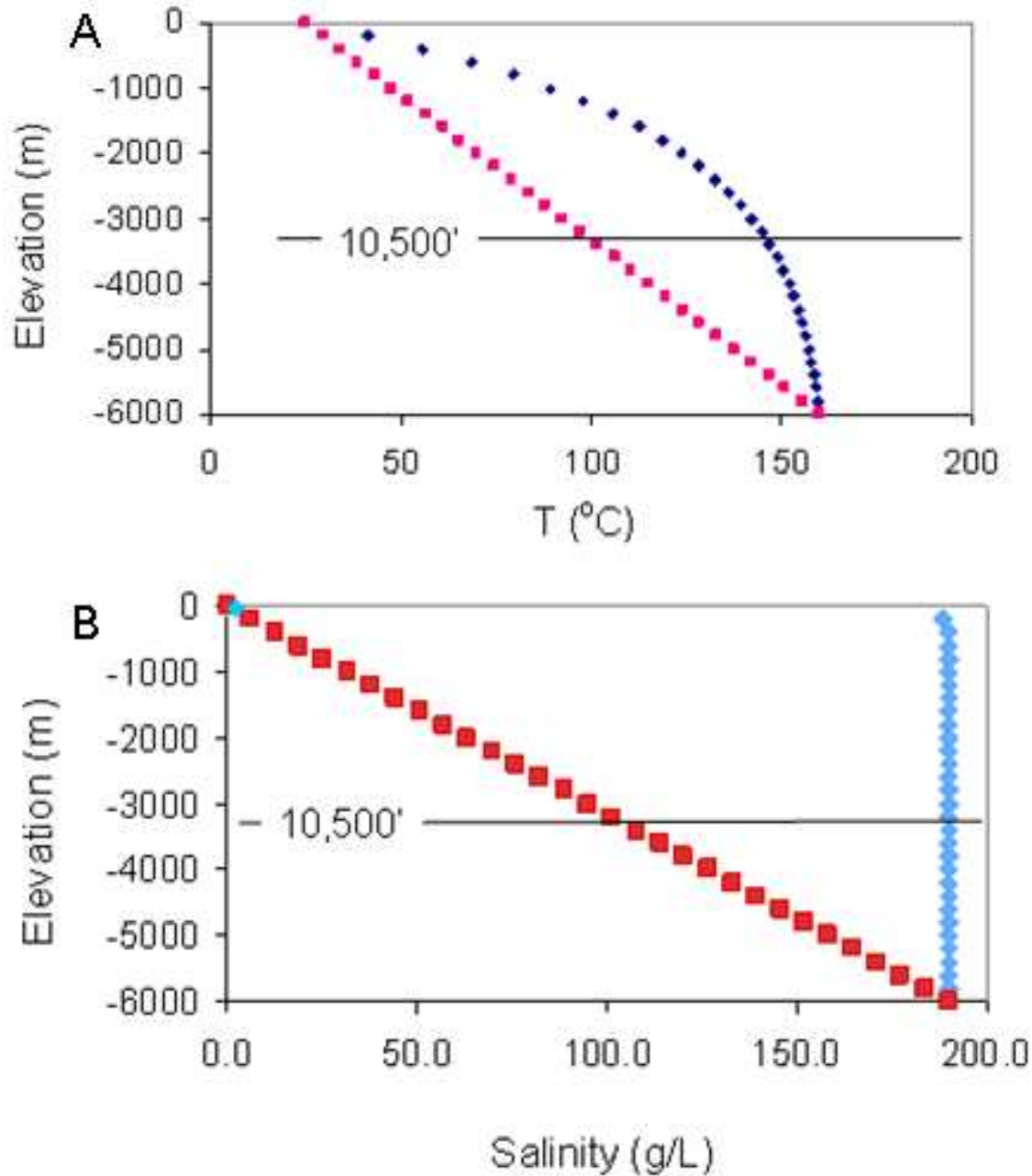
Figure 4.7. A: Graph of hypothetical steady-state vertical heat transport. The red line indicates the change of temperature with depth due only to thermal conduction as a mechanism of heat transport. The blue line shows change in temperature with depth with an upward fluid flow velocity of 2.4 cm/y in addition to conduction. B: Graph of hypothetical vertical solute transport. The red line indicates the change in salinity by molecular diffusion alone. The blue line shows the change in salinity with both fluid flow and molecular dispersion. The decrease in temperature at shallow depths by conduction is much more rapid than the decrease in salinity by molecular diffusion.

smaller area of West Baton Rouge Parish at a depth of 1,000 ft (300 m) (Figure 4.9 B). Areas to the east of the river also show the presence of fresh water in the saltwater zone, particularly at a depth of 500 ft (150 m) (Figure 4.9 A).

The large saline plume extending northwest from the St. Gabriel salt dome is not present below 1,000 ft (300 m), and freshwater plumes present to the south of the Baton Rouge fault become more pronounced and stretch farther into the salt water zone in narrow plumes (Figure 4.9 C-F). Small amounts of saltwater exist on the south side of the fault directly east of the Mississippi River at 1,500 and 2,000 ft (450 and 610 m) depths (Figure 4.9 C-D) in addition to larger areas west of the river at 1,500, 2,500, and 3,000 ft (450, 760, and 910 m) depths (Figure 4.9 C, E, and F) with a small, relatively salty plume (20 g/L) extending northeast from the area of the Bayou Choctaw and Bayou Blue salt domes.

Three salinity cross sections were created through the regional study area, two running from west to east, and one from north to south (Figure 4.8). Cross section A-A' (Figure 4.10) is located north of the major salt water plume, and shows the variations in salinity at a distances of 0.5-3 miles (0.8-5 km) to the south of the Baton Rouge fault. The eastern side of cross section A-A' shows an area of freshwater present both above and below a plume of salty water, with an area of relatively freshwater (0-0.5 g/L) present at the shallowest 1,000 ft (300 m) overlying saltwater (10-50 g/L) that is present north of the St. Gabriel salt dome at a depth interval of 1,000-2,500 ft (300-760 m). Another area of freshwater (0.2-0.5 g/L) from the north occurs in the 2,500-3,000 ft (760-910 m) depth interval. Most of the remaining waters in this cross section have mid-range salinities (1-10 g/L) with a few areas of relative freshwater (0.2-0.5 g/L) in the middle of the section, which is an area located very close to the fault. One area of high salinity (20-150 g/L) is located at a depth of 3,000 ft (910 m) in the middle of the section.
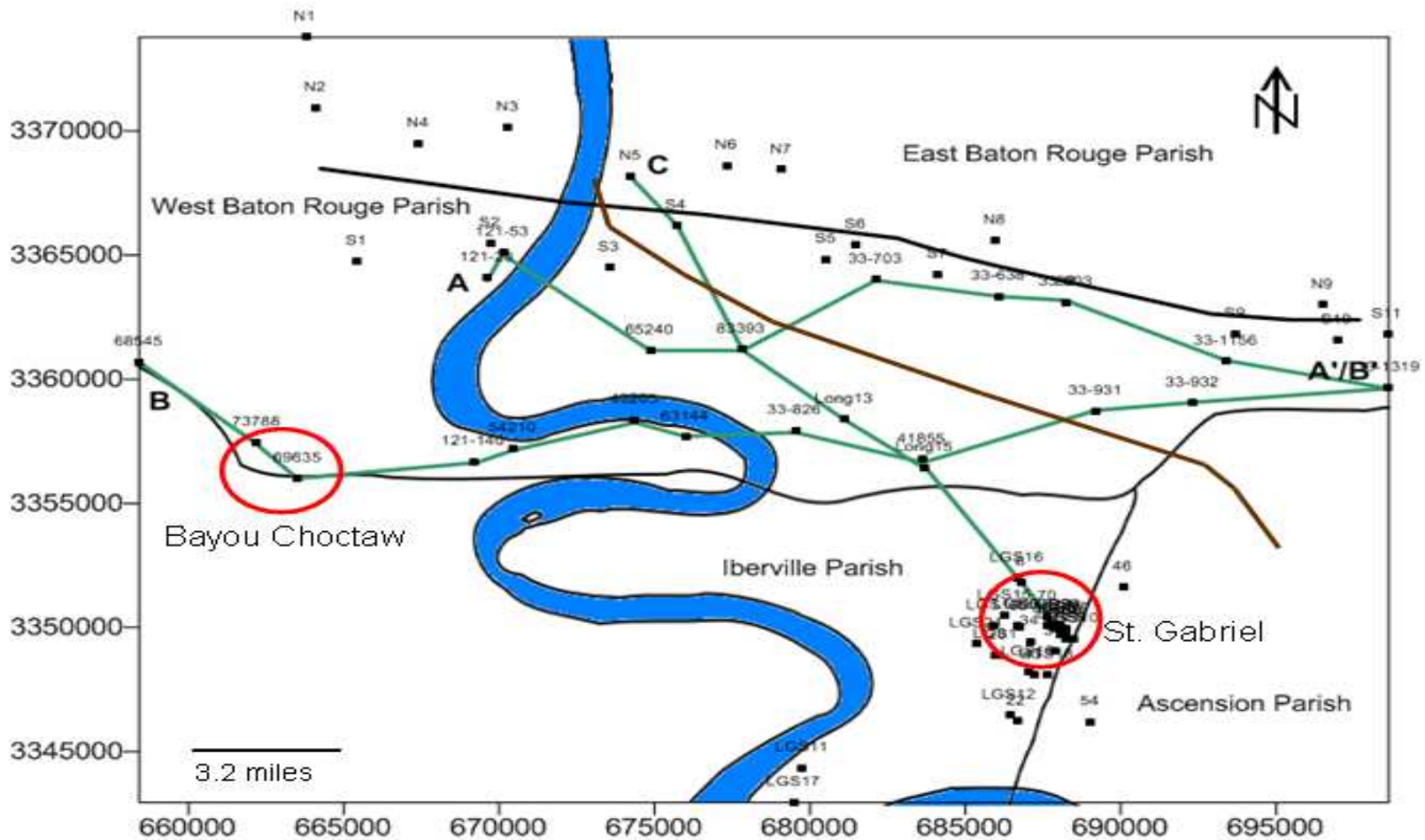
Figure 4.8. Map showing the regional study area. Black dots show locations of boreholes used in the regional study. Red circles show locations of the salt domes with the study area, the Bayou Choctaw and St. Gabriel fields. The bold black line is the Baton Rouge fault. The brown line is the division between the Mississippi River alluvial aquifer to the south and the Baton Rouge aquifer system to the north. Green lines show locations of cross-sections created in the study. Location grid is in UTM coordinates.
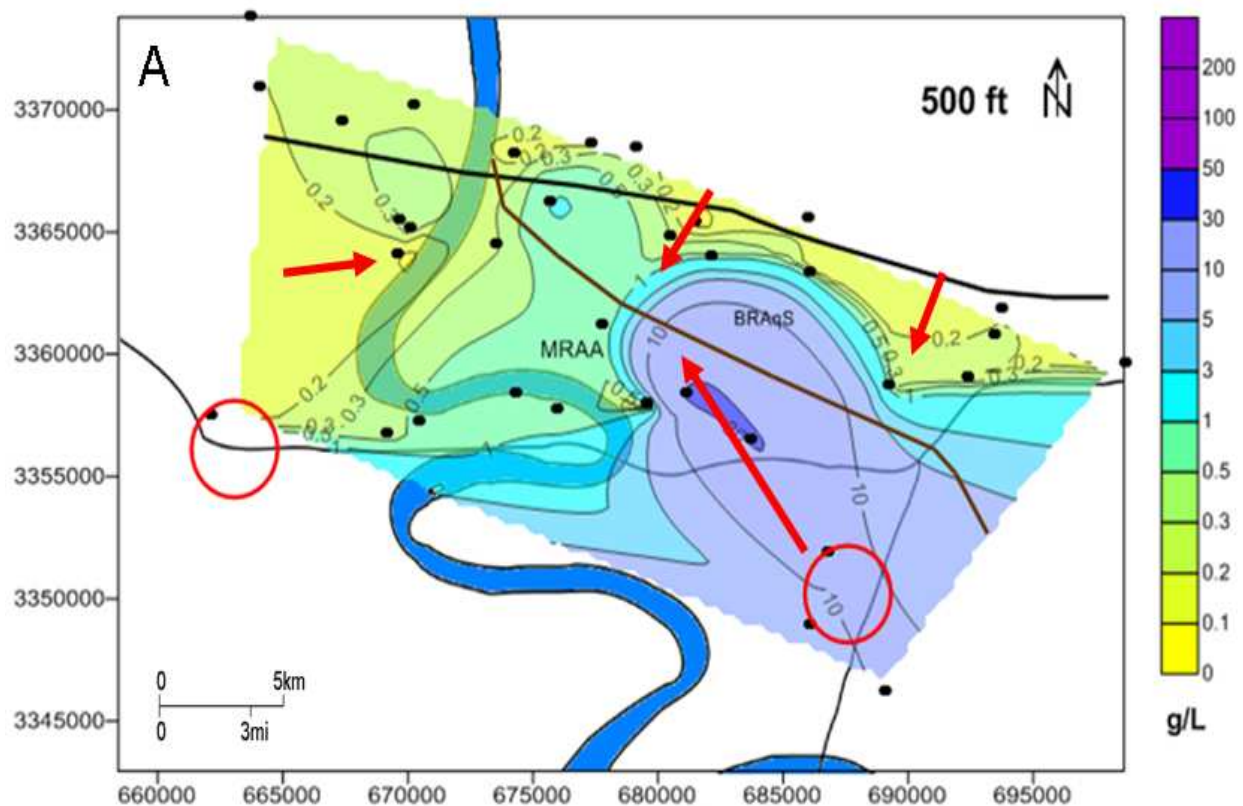
Figure 4.9 A-F. Contour maps showing spatial variations of salinity on a regional scale for varying depths at 500 ft intervals. Based on regional map (Figure 4.8). Black line is the Baton Rouge fault. Brown line in figures A and B represents the eastern edge of the Mississippi River Alluvial Aquifer. Red arrows show in inferred directions of past fluid flow based on spatial variations in salinity. It is assumed that fresher waters were sourced from the north and that saline waters were sourced from salt domes to the south. Note logarithmic scale for salinity. For reference, the approximate upper salinity limit for potable water is 0.5 g/L and the average salinity of seawater is 35 g/L.

(Figure 4.9 continued)
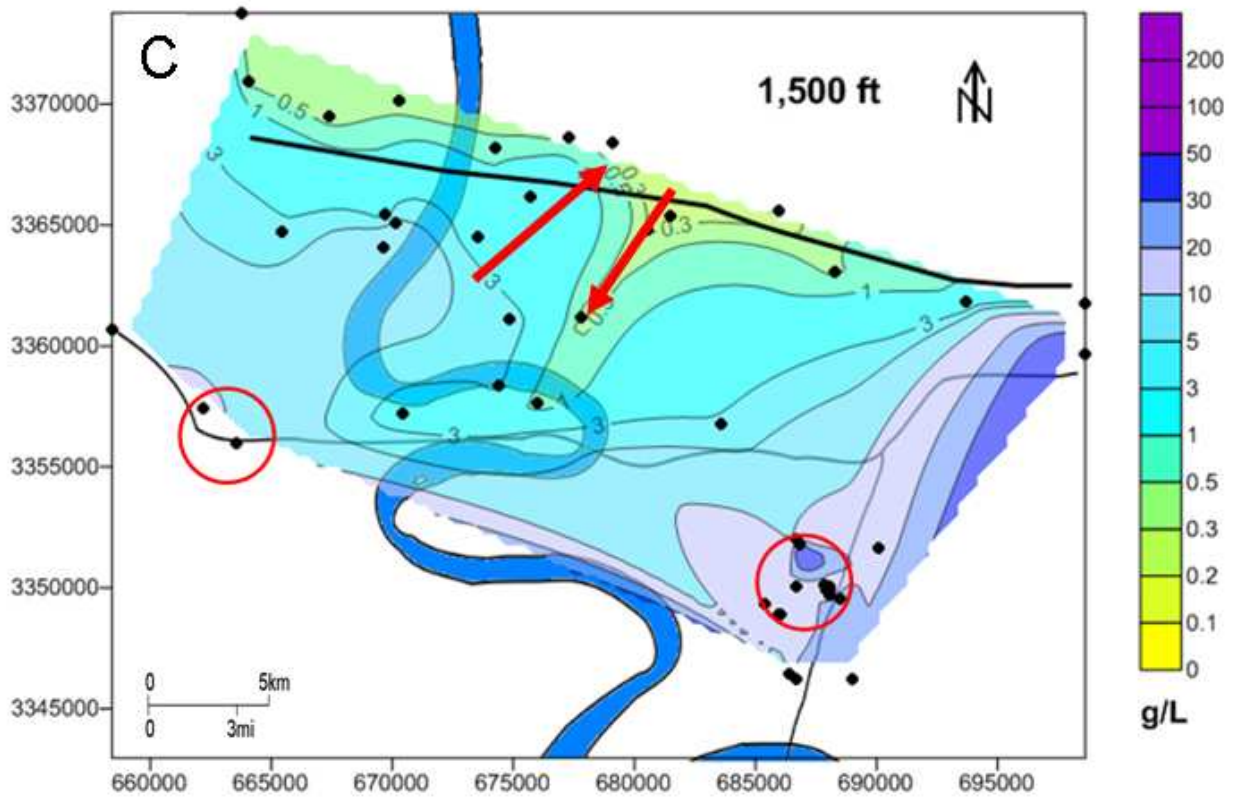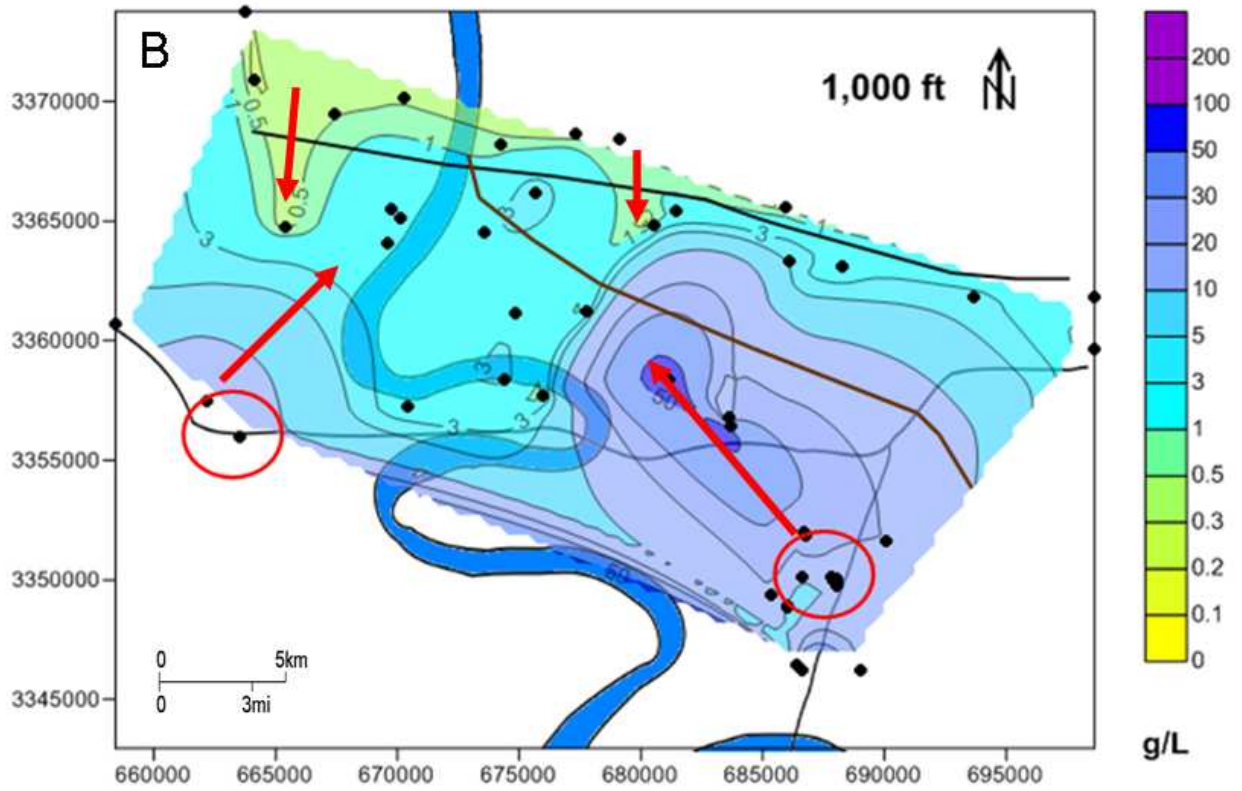
(Figure 4.9 continued)
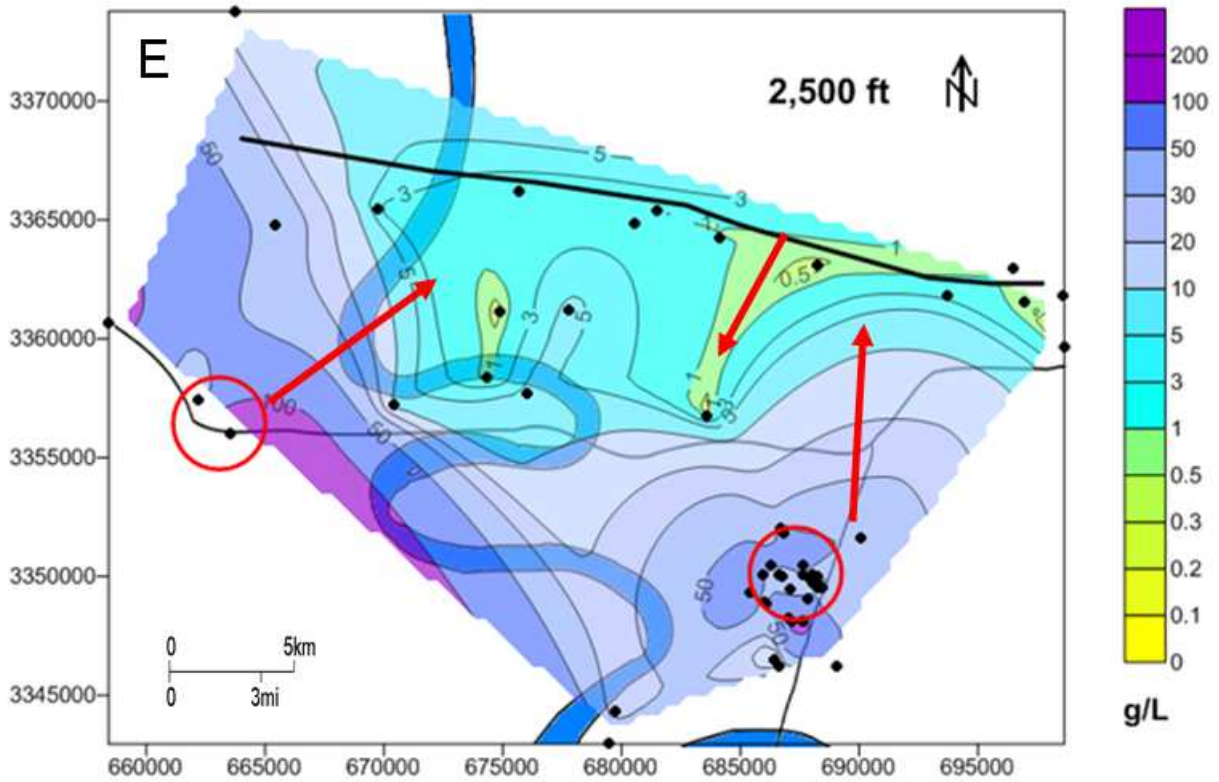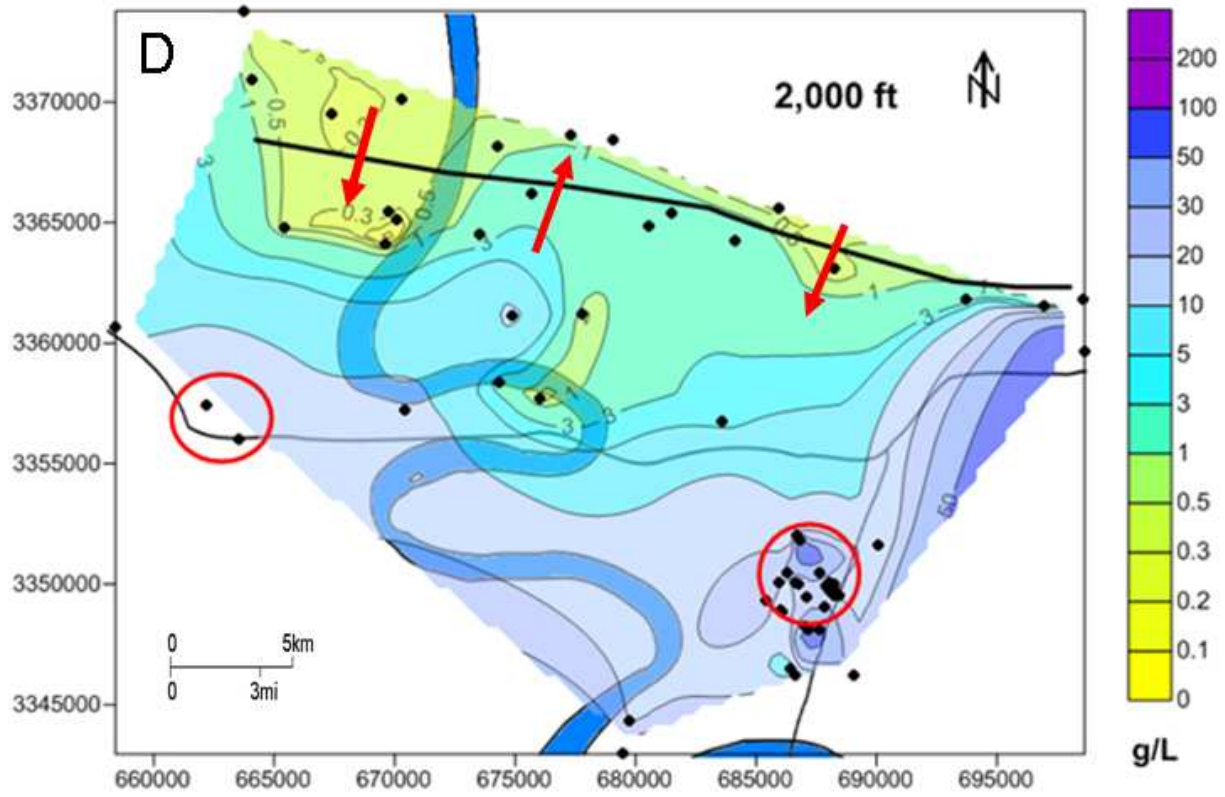
(Figure 4.9 continued)
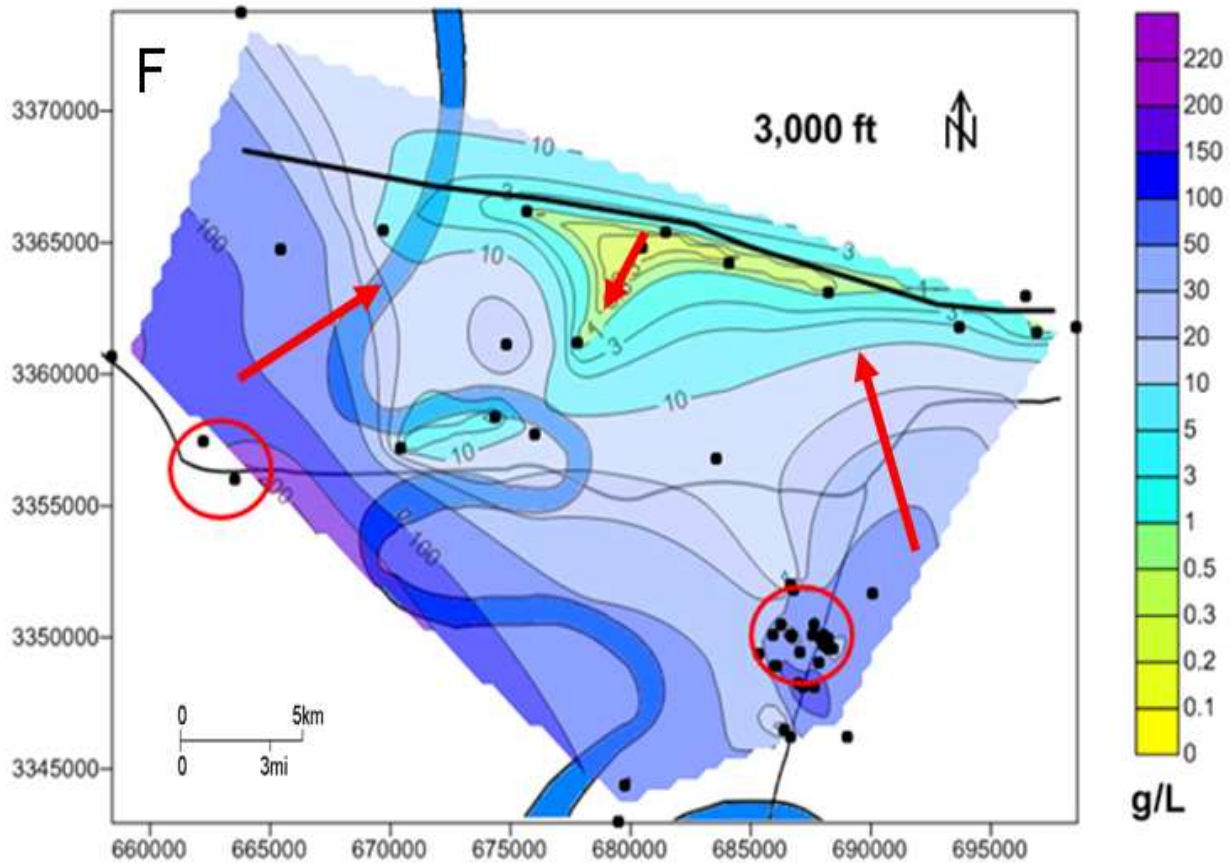
Salinity cross section B-B' (Figure 4.11) traverses the entire regional field study in a west-east direction at a varying distance of 2-8 miles (3-12 km) south of the fault (Figure 4.8). There are two high salinity areas in the section. One is on the western side of the Mississippi River is located near the Bayou Choctaw salt dome, and has salinities between 20-150 g/L. The other high salinity plume is located on the eastern side of the cross section, north of the St. Gabriel field area and has salinities of between 20-100 g/L. The middle section contains waters of lower salinities (1-10 g/L). A small area of freshwater is present on the eastern side of the cross section in the top 1,000 ft (300 m).
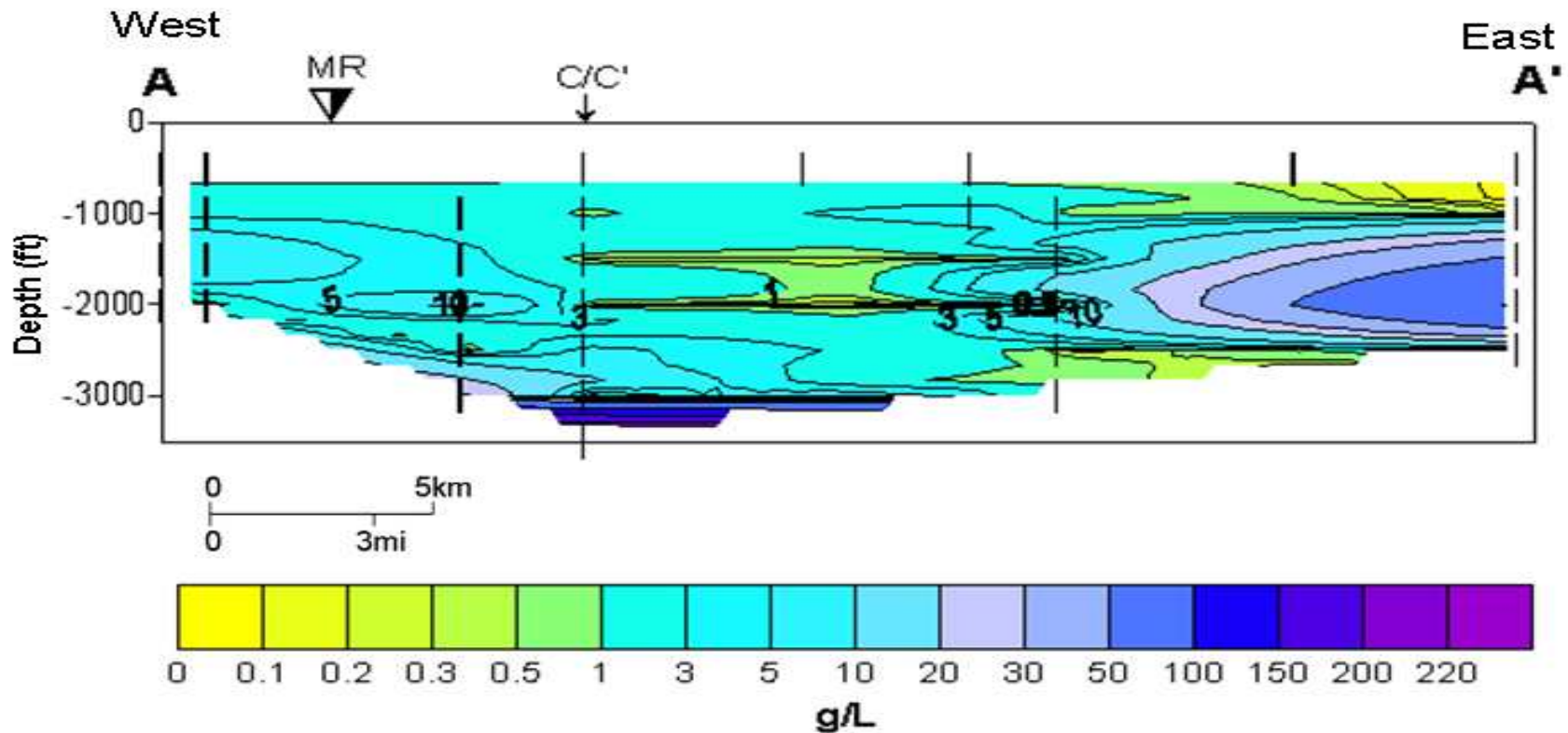
Figure 4.10. Cross section A-A' illustrating the spatial variations in salinity from the regional study area. MR shows the location of the Mississippi River. C/C' shows the well which intersects with cross section C-C' (Figure 4.12). Locations of cross section lines are shown in Figure 4.8. Note logarithmic scale for salinity. For reference, the approximate upper salinity limit for potable water is 0.5 g/L and the average salinity of seawater is 35 g/L.
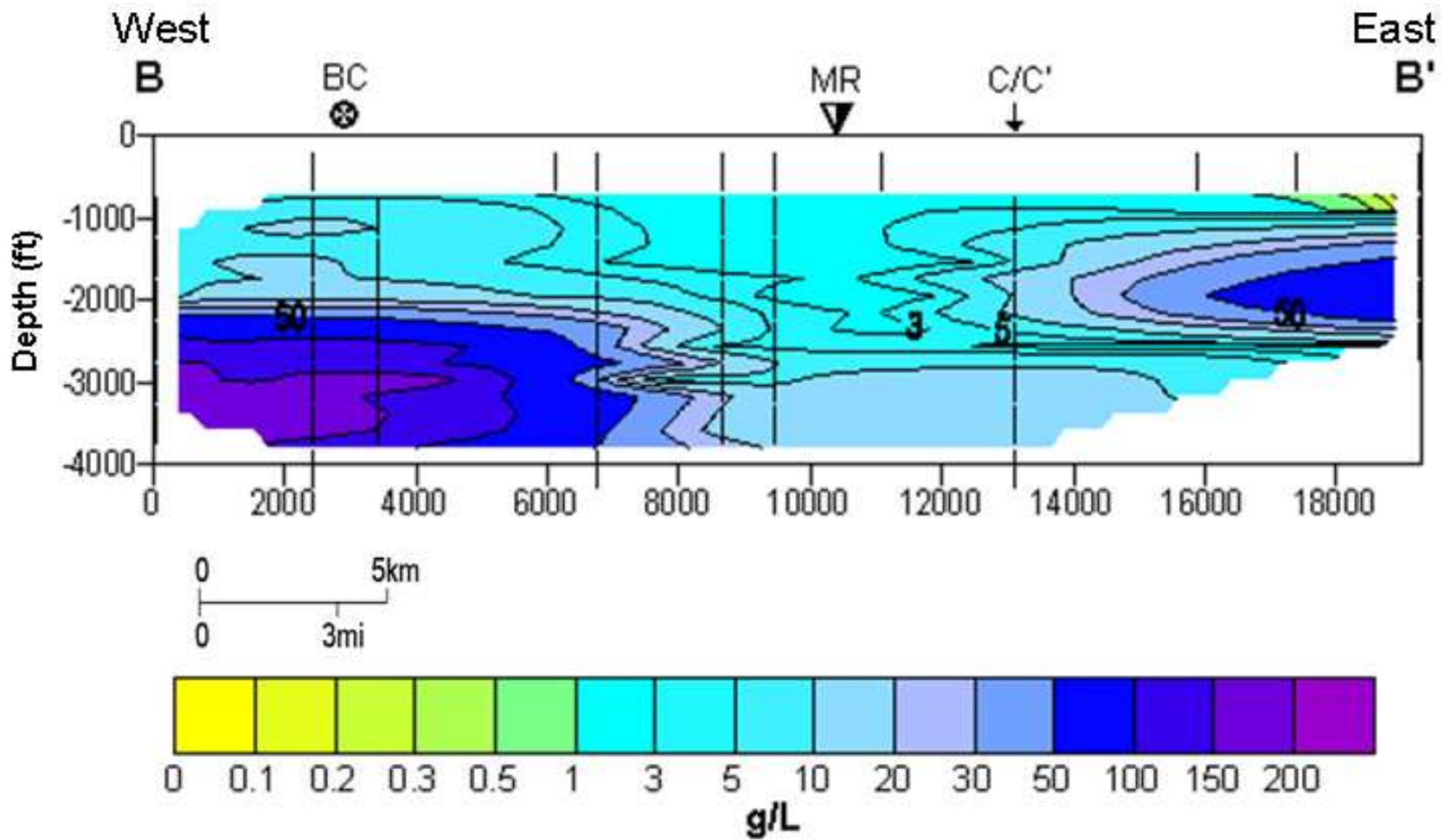
Figure 4.11. Cross section B-B' illustrating spatial variations in salinity. BC shows the location of the Bayou Choctaw dome, MR shows the location of the Mississippi River, and C/C' shows the location of the well that intersects the C-C' cross section (Figure 4.12). The location of the cross section line can be seen in Figure 4.8. Note logarithmic scale for salinity. For reference, the approximate upper salinity limit for potable water is 0.5 g/L and the average salinity of seawater is 35 g/L.
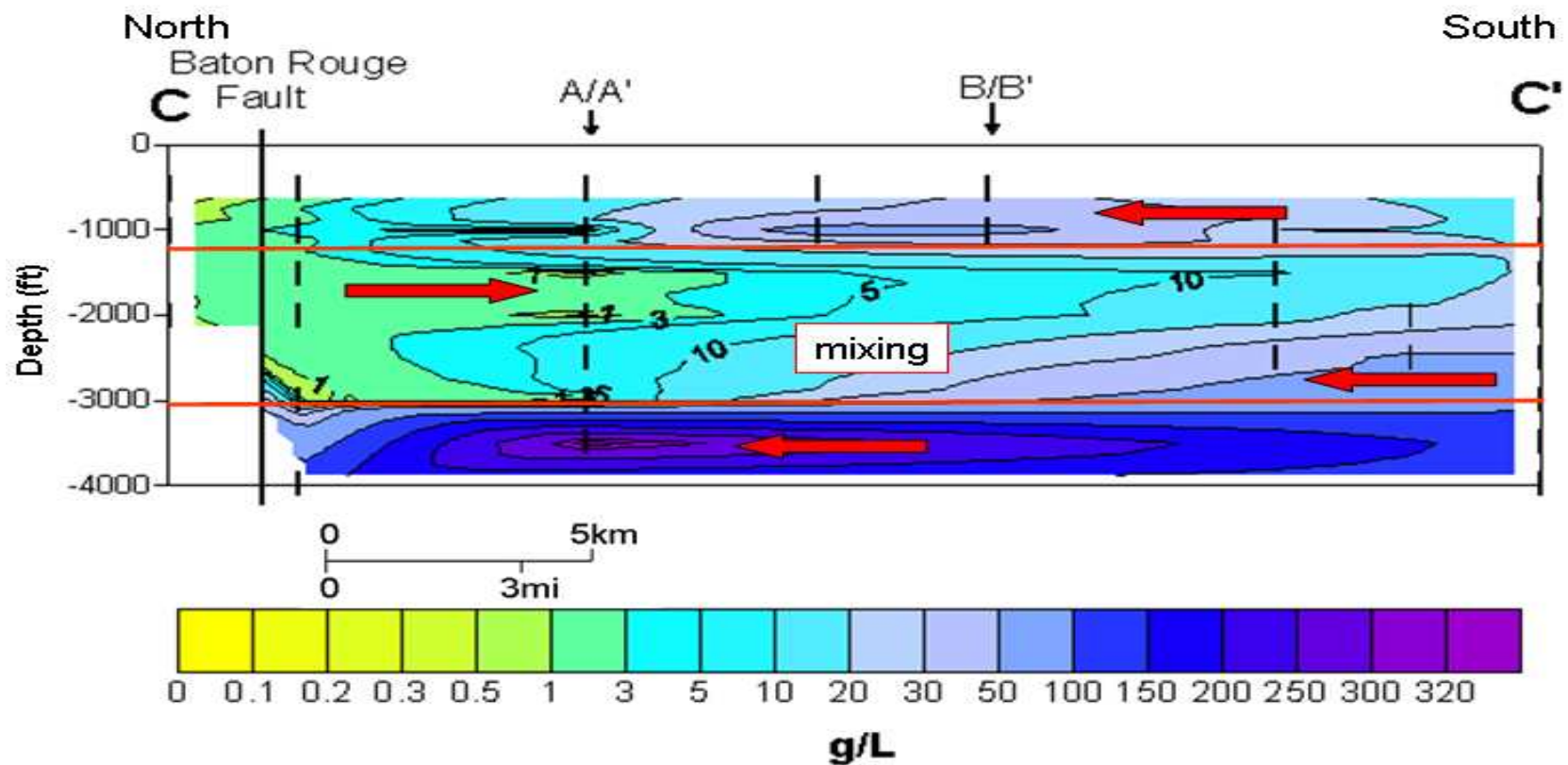
Figure 4.12. Cross section C-C' illustrating spatial variations in salinity. The location of the Baton Rouge fault is labeled. A/A' and C/C' show boreholes that intersect with cross sections A-A' (Figure 4.10) and B-B' (Figure 4.11). Red arrows show directions of fluid flow. The location of the cross section line is show in Figure 4.8. Note logarithmic scale for salinity. For reference, the approximate upper salinity limit for potable water is 0.5 g/L and the average salinity of seawater is 35 g/L. Note poor well control to the north of the fault, so the reaction of the contours south of the fault decreasing in salinity as they approach the fault is an artifact of contouring. Figure 1.4 shows that this area of high salinity continues to the north of the fault.

Salinity cross section C-C' (Figure 4.12) runs across the regional field study from approximately north to south. The section shows three distinct zones. The deepest zone, the interval below 3,000 ft (910 m) has high salinities between 30-300 g/L, and extends north from the St. Gabriel field. The middle zone, between a depth of 1,500-3,000 ft (450-910 m), contains much less saline water (0.3-10 g/L), which extends from north of the fault to the south and overlies a wedge of more saline waters (20-100 g/L) which extends northward from the St. Gabriel area. The uppermost zone, between 500-1,500 feet (150-450 m), has relatively high salinity waters (20-50 g/L) which extend from the St. Gabriel field toward the north through the shallow sands of the Mississippi River Alluvial Aquifer.

Density

Calculations of *in situ* densities were made for waters in the C-C' cross section (Figure 4.13). The spatial variations in densities generally correlate with the spatial variations in salinity (Figure 4.12). Areas of high salinity correspond with areas of high density and low salinity areas correspond with areas of low density. The topmost section, the interval between 500-1,500 feet (150-450 meters) has waters of higher densities, in the range of 1,020-1,040 kg/m^3. The middle interval, between 1,500-3,000 ft (450-910 m), has much lower densities (980-1,010 kg/m^3) than the lower zone. A large section within the middle zone exhibits a flat density field where little density change occurs. The lower zone below 3,000 ft (910 m) has waters of very high densities in the range of 1,040-1,130 kg/m^3.
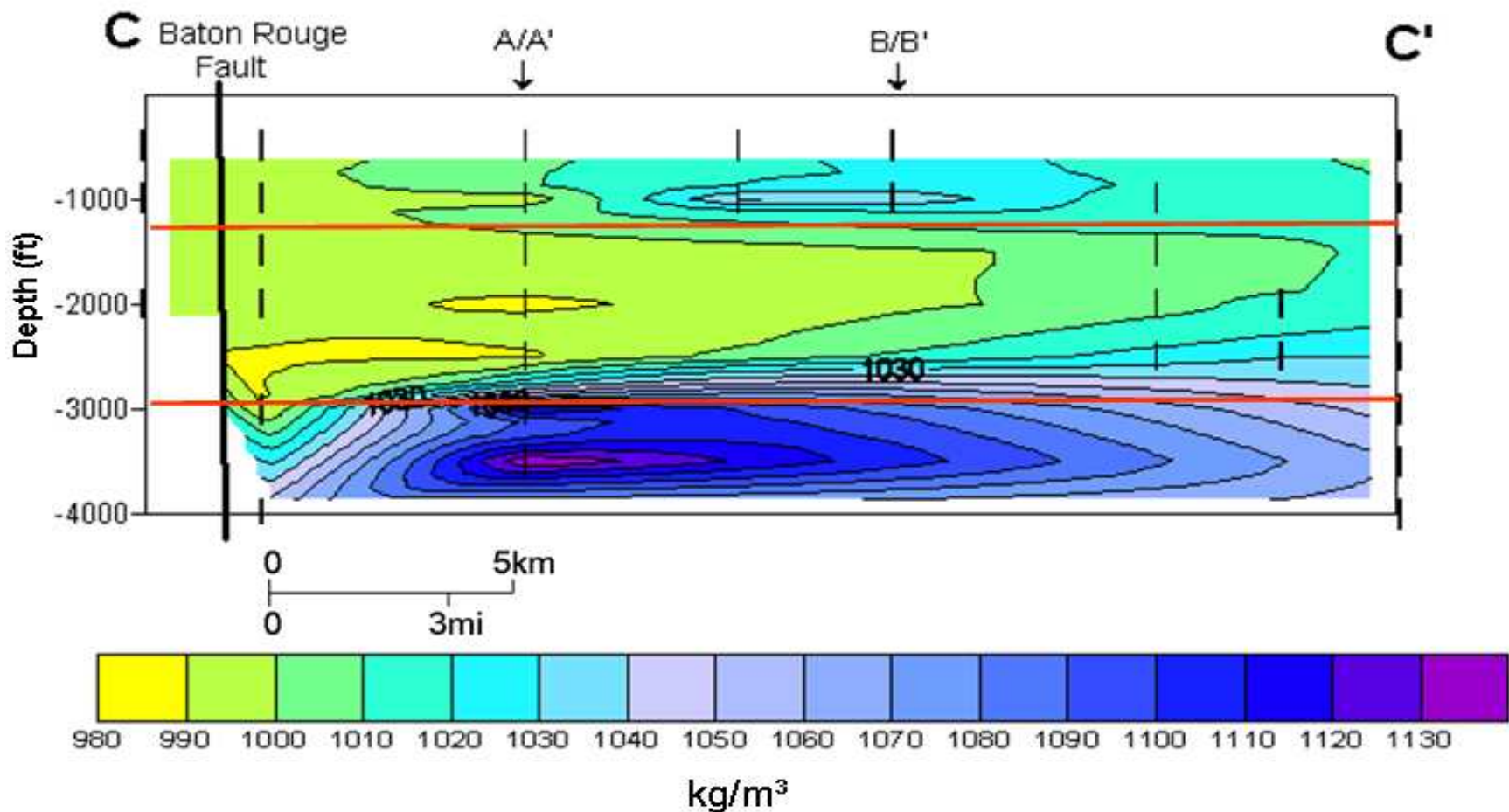
Figure 4.13. Cross section C-C' illustrating spatial variations of *in situ* fluid density corrected for pressure, temperature, and salinity along cross section C-C' in the regional study area. The location of the Baton Rouge fault is shown. A/A' and B/B' show locations of boreholes that intersect with cross sections A-A' (Figure 4.11) and B-B' (Figure 4.12). The location of the cross section line is visible in Figure 4.8. Note poor well control to the north of the fault, so the reaction of the contours south of the fault decreasing in density as they approach the fault is an artifact of contouring. Figure 1.4 shows that the area of high salinity continues to the north of the fault, so the area of high density likely follows this pattern.

DISCUSSION

The St. Gabriel Field

The highest salinities in the St. Gabriel field occur in an annular area around the apparent crest of the domal structure for a large portion of the depth interval studied (Figure 4.1, C-H). The highest salinities occur in the center of the plumes, particularly in the deeper sections, and decrease both laterally and upward, as illustrated by the cross section across the dome (Figure 4.2). The spatial variations in apparent temperature gradient show a similar trend, with the higher apparent temperature gradients around the edges of the domal structure and a relative low over the top of the dome (Figure 4.3). As previously discussed the salinity and apparent temperature gradients show a general, but not perfect, correlation, suggesting that variations in the two are related.

These spatial variations of saline waters and temperature support the conclusion that upward transport of heat and salty water is occurring or has occurred locally at the St. Gabriel salt dome, as an explanation for the temperature and salinity anomalies at relatively shallow depths. The heat transport equation by Bredehoft and Papadopulos (1965) was used, as previously discussed, to assess steady-state vertical transport as a possible explanation. When a fluid velocity of 2.4 cm/year for fluid flow is paired with thermal conduction, the results produce a non-linear variation in temperature (Figure 4.6, A). This may explain the presence of the high temperature gradients at relatively shallow depths. If there were no vertical fluid flow, and the only heat transport mechanism were conduction, there would be a linear increase in temperature with depth, and the high temperatures observed at relatively shallow depths would not exist.

To examine the mechanics of vertical solute transport, an equation by Finlayson (1992) was used, as previously discussed. Using a true fluid velocity of 2.4 cm/year, the calculations

produce high salinity readings with very little change with depth, until very shallow depths where salinity drastically decreases (Figure 4.6, B). The red line (Figure 4.6,B) shows molecular diffusion as a transport mechanism alone with no fluid advection. Molecular diffusion alone would produce a steady, linear decrease in salinity with decreasing depth, which does not match the findings at St. Gabriel. Calculations showing the combination of fluid flow and dispersion is broadly similar to some of the salinity profiles from the St. Gabriel field (Figure 5.1) (Appendix I).

The results from these idealized vertical transport models and the patterns seen in the spatial variations in both salinity and apparent temperature gradient at the St. Gabriel field suggest that some process of vertical advective transport of heat and solutes is occurring or has occurred. However, the steady-state model calculations represent hypothetical conditions, and actual transport will likely be more complex in reality. It is possible that the vertical transport is related to faults associated with the salt dome (Figure 2.2). These complex normal faults may act as fluid conduits, creating vertical pathways for the migration of warm, saline water.

Other salt domes have documented evidence for vertical solute transport above salt. One example is the Welsh dome in Jefferson Parish, southwestern Louisiana. A study of the Welsh dome by Bennett and Hanor (1987) showed the presence of a plume of highly saline water, with salinities exceeding 160 g/L (Figure 5.2). This saline plume extends one kilometer (3,280 ft) vertically above the dome, and several kilometers laterally. In addition, there is a temperature anomaly of high temperatures that is approximately spatially coincident with the observed salinity highs. Other similarities of the Welsh dome to the St. Gabriel field includes an overpressured zone, thought to possibly be causing fluid migration upward. The previously
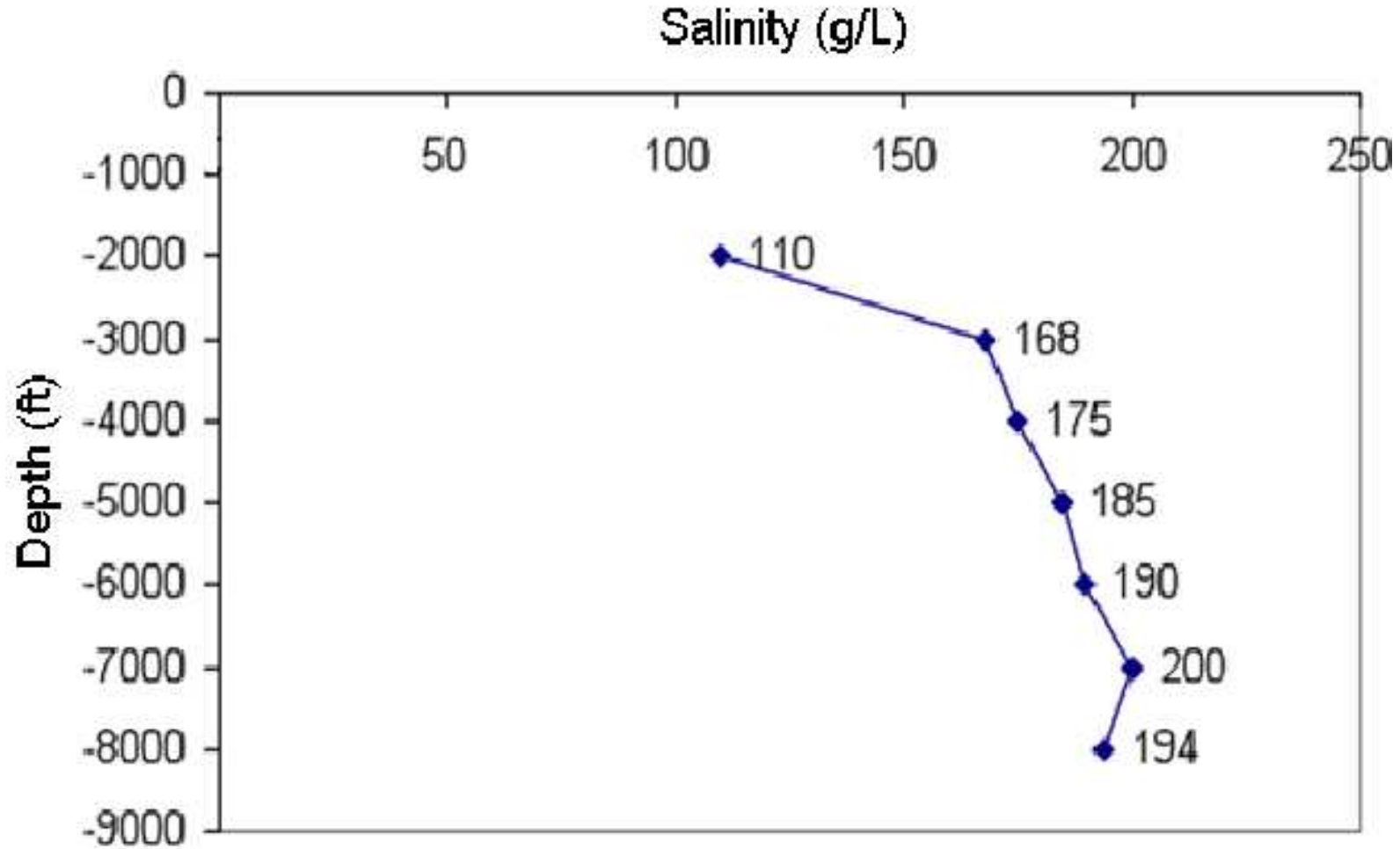
Figure 5.1. A graph showing the change of salinity with depth from borehole 41 from the St. Gabriel field. The groundwater maintains relatively high salinities upward until reaching approximately 2,000 feet in depth, where a large decrease in salinity occurs. Location of borehole 41 can be found in Appendix I.

discussed patterns in salinity and apparent temperature gradient around the St. Gabriel field may have also been caused by a dewatering event.

Williams and Ranganathan (1994) developed a solute transport and heat transport model for a transient dewatering event of an overpressured zone adjacent to a salt stock, and showed that the long-lasting effect on the salinity and temperature fields that can potentially exist thousands to even millions of years after the depressurizing event. The results of their calculations (Figure 5.3) show the formation of high salinity plume caused by dissolution of salt associated with the dewatering event, which grows outward from the original discharge point, and which eventually collapses on itself and flattens out. However, even as long as several million years later, a high salinity zone is left as evidence of this past event. Williams and Ranganathan also modeled the effect of the fluid expulsion on temperature during a dewatering event (Figure 5.4). There is a spike in the isotherms at the zone of fluid expulsion which grows and eventually dissipates over approximately 100 thousand years. The results produced by this model broadly compares to findings from the St. Gabriel field. The high salinity plumes from the St. Gabriel field (Figure 4.2), along with the high apparent temperature gradients, occurring annularly around the top of the structure may be the result of past dewatering events from the overpressured zone. Roberts and Nunn (1995) also applied a numerical model to the dynamics of expulsion events from overpressured zones. Their study concluded that expulsion events are part of a complex process that takes 10,000 to 500,000 years.

Areas at St. Gabriel where high apparent temperature gradient is not associated with an area of high salinity (Figure 4.4) may be due to advective movement of warm waters that have not come in direct contact with salt. Because temperature anomalies dissipate faster than salinity
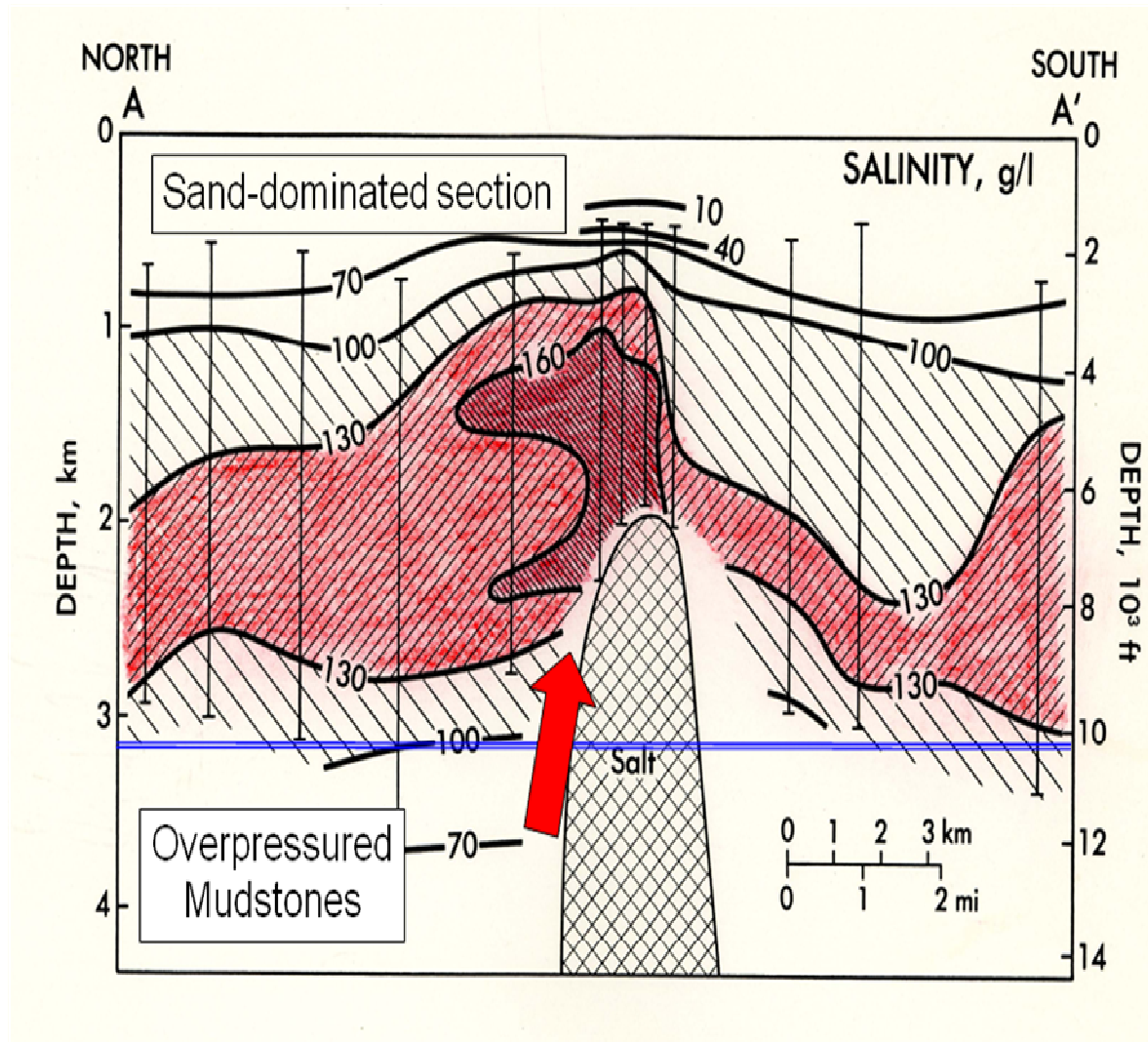
Figure 5.2. A cross section of the Welsh field in Jefferson Parish, Louisiana, showing the location of a vertical salinity plume extending above the Welsh dome (modified from Bennett and Hanor, 1987). The red arrow represents a possibly fluid expulsion event from the overpressured zone, and the blue line shows the top of overpressure.
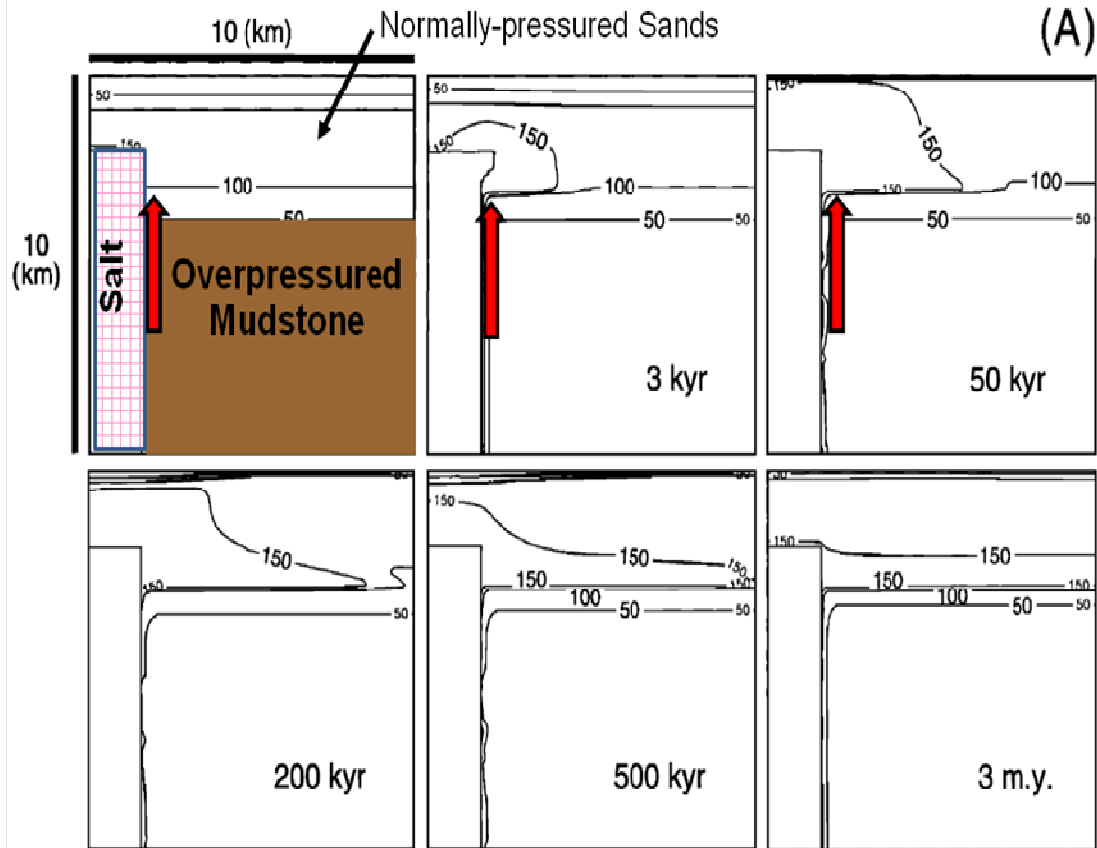
Figure 5.3. A model created by Williams and Ranganathan (1994), showing the calculated effects of a dewatering event near a salt dome on spatial variations in salinity over time. Dissolution of salt produces a perched salinity plume which eventually collapses on itself. Compare with plumes at St. Gabriel (Fig. 4.2) and Welsh (Fig. 5.2.)
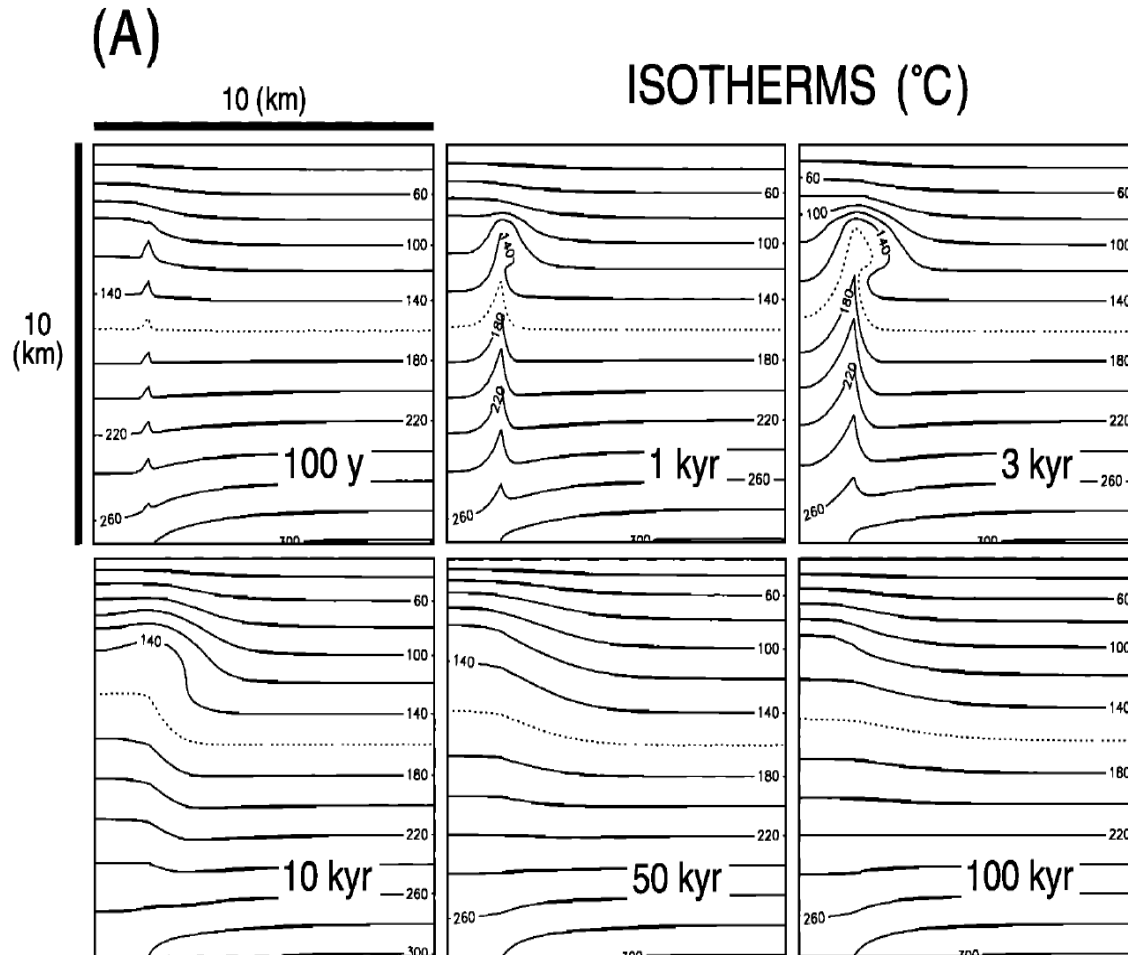
Figure 5.4. Model created by Williams and Ranganathan (1994) showing the calculated effects of an episodic upward dewatering event on the thermal field in the vicinity of a salt dome.

anomalies, a general assumption based on the Williams and Ranganathan (1994) models can be made that the dewatering events would have occurred less than ten thousand years ago, which also seems to match the modeled salinity patterns with plumes occurring at the St. Gabriel field (Figure 5.3 and 5.4).

The Baton Rouge Aquifer System and the Baton Rouge Fault

For the purposes of interpreting the results this study, the assumption will be made that saltwater in the study area has originated south of the Baton Rouge fault and that freshwater has originated from north of the fault. A main source of the saltwater which has moved northward into the area south of the Baton Rouge fault appears to be the St. Gabriel dome. Large areas of relatively high salinity groundwater has moved northwest from St. Gabriel, particularly expressed by the shallower slice maps (Figure 4.9 A,B). These salty waters may be related to the previously mentioned vertical transport occurring locally at the St. Gabriel field. This northwest-trending plume is not present in the deeper sections. The location of this plume may be explained by the presence of the MRAA. Saline waters moved up the faults associated with the dome (Figure 2.2) and were then available to move laterally through the sands and gravels of the Mississippi River Alluvial Aquifer. The MRAA has thus acted as a channel for the northern movement of saline water (Figure 2.5).

The thick layers of sand of the MRAA show generally high resistivity throughout much of the sand packages, with a change to lower resistivity at the base of the unit (Figure 2.6). This change suggests that salinity is stratified within the aquifer, with the fresher waters present at the top, and saltier waters present at the base. At the location of borehole 121-53 (Fig. 2.6) very high salinities are also present in an older Pleistocene sand underlying the MRAA at depths of 750 to 800 ft (230 to 240 m), indicating that highly saline waters have leaked downward into

underlying sediments from the MRAA salinity plume. The next sand down at a depth of 1,000-1,100 ft (300-335 m) has less saline water in it, as evidenced by a smaller SSP response and a higher resistivity. The difference in densities between fresh and saline waters may be a driving force for the northward movement of saline waters. In addition to the MRAA, several individual sand units at varying depths show this stratification of salinities, and therefore the possibility of density-driven fluid flow (Figure 5.5). Similar evidence for salinity stratification in aquifer sands in the Baton Rouge area was reported by Carlson (2008). However, not all sand units show this stratification of salinity (Figure 5.6).

There are also several areas within these shallow sections where relatively fresh water has moved south. As shown by the red arrows, southward movement of fresh waters has occurred at several different places across the fault at depths of between 500 and 1,000 ft (150-460 m) (Figure 4.9 A,B).

Beginning at depths of 1,500 feet (450 m), the salinity pattern changes. At depths of 1,500 and 2,000 ft (450 and 600 m) larger areas south of the fault have waters of mid-range salinities (1-10 g/L) (Figure 4.9 C,D). There are several locations where freshwater has moved south of the fault, creating long freshwater tongues into the saltwater zone (Figure 4.9 C). Relatively salty waters have also moved northward across the fault. Higher salinities at these depths are beginning to be evident on the western side of the study area, near the vicinity of the Bayou Choctaw salt dome. The Bayou Choctaw dome is located on the boundary between Iberville and West Baton Rouge Parishes, with a relatively shallow depth (630 feet/190 meters) to the top of salt (Welch and Hanor, 2011) (Figure 1.1) This dome may be the major salt source

SP (millivolts)   Resistivity (ohms)

Fresh water

Brackish water

borehole 49205

SP (millivolts)   Resistivity (ohms)

Fresh water

Brackish water

Borehole 033-803
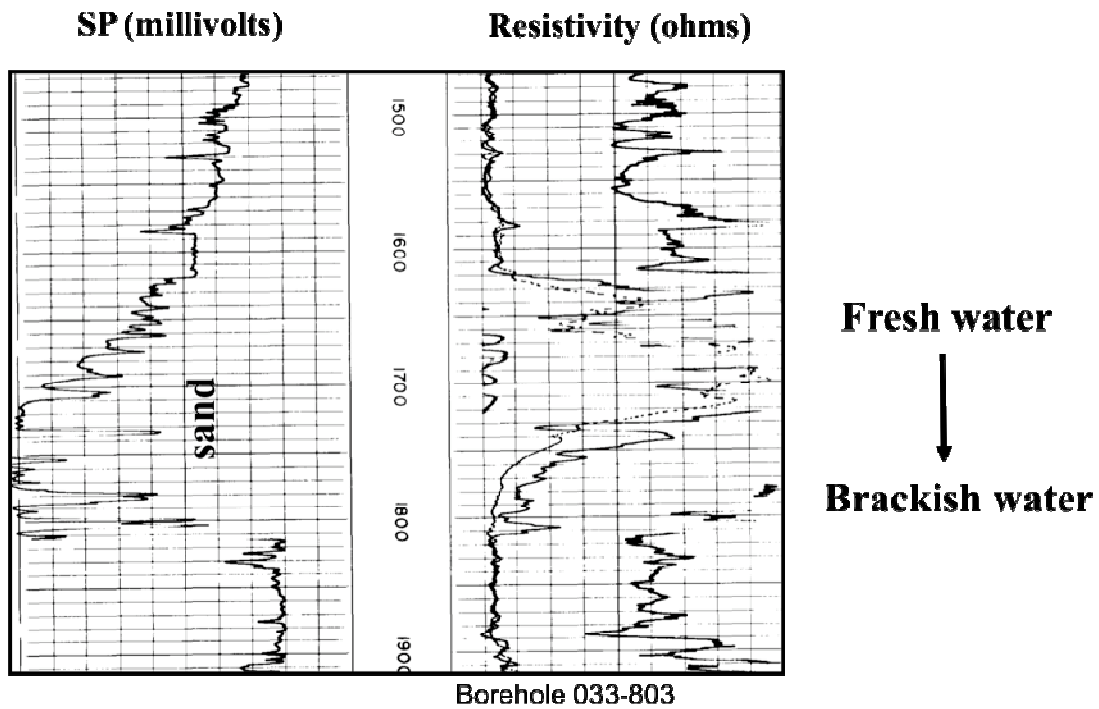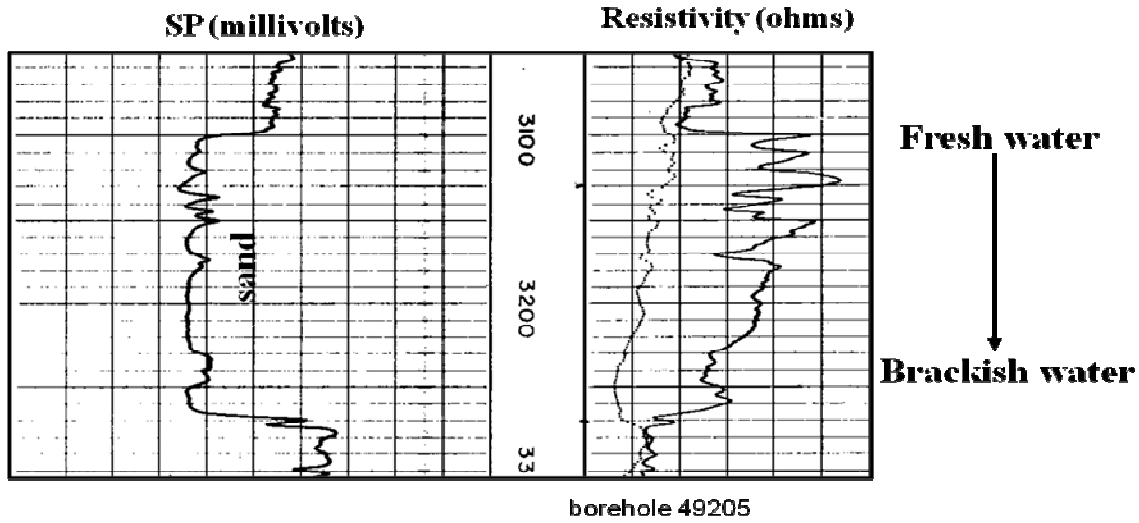
Figure 5.5. Borehole logs for individual sands showing a stratification of salinity within the units. High resistivity at the top of the unit indicates relatively fresh water. The resistivity decreases towards the base of the unit, which indicates that the water is becoming increasingly brackish towards the base.

55
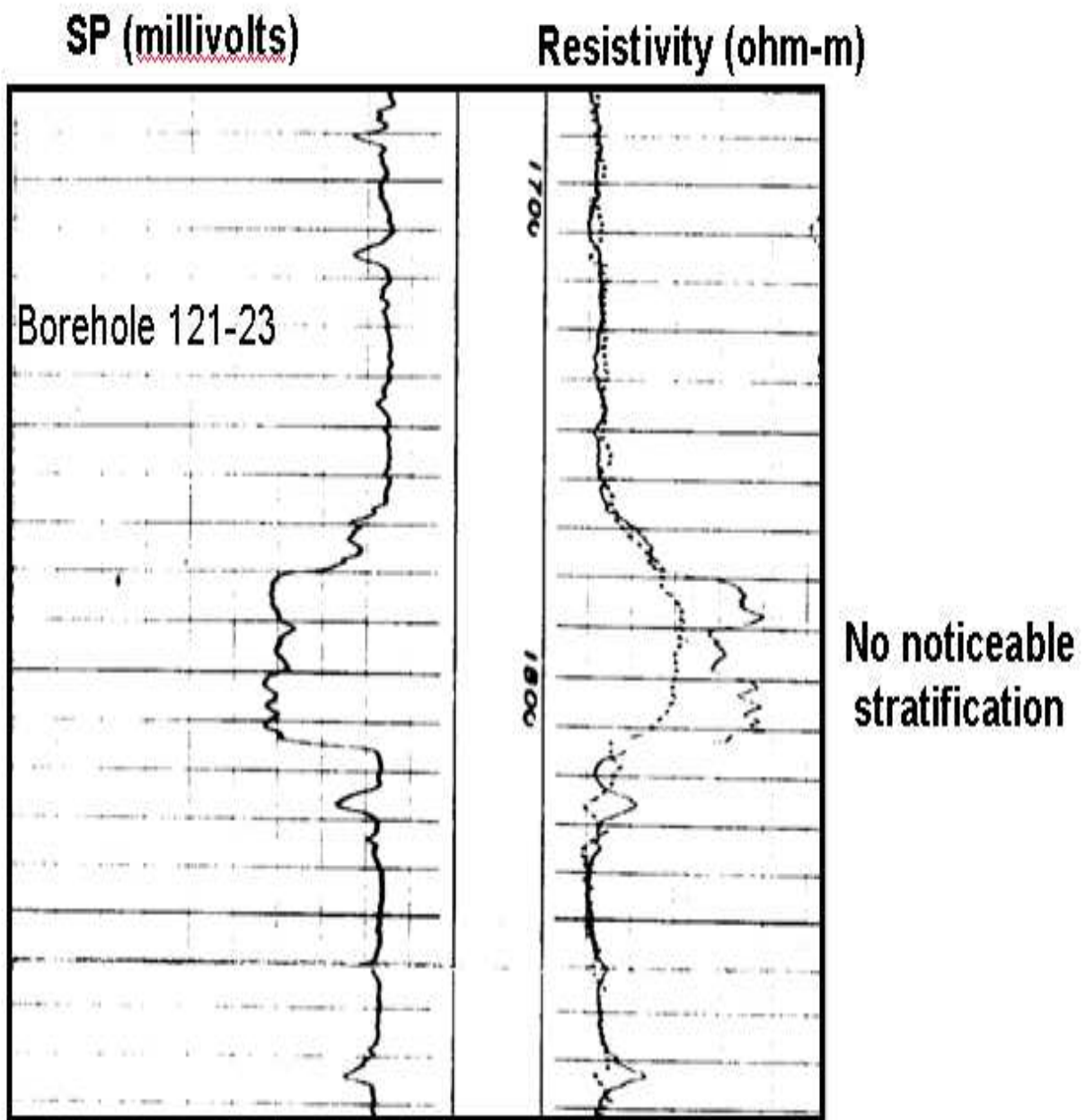
Figure 5.6. Bore log for an individual sand showing no stratification of salinity.

for the increased salinity in the area as well. However other salt domes out the range of the study area, such as Bayou Blue or White Castle domes, may also be contributing to high salinities south of the fault (Figure 4.9 C,D).

The two deepest sections, at depths of 2,500 and 3,000 ft (760 and 350 m), shows an increase in salinity over large portions of the study area (4.9 E,F). The western side of the study area in particular shows the presence of waters of very high salinities that have moved northeastward toward the area south of the fault. These highly saline waters may be from the Bayou Choctaw dome and other salt structures to the west. High salinities also extend north from the St. Gabriel field, as shown by red arrows. Despite the increase in salinity over most of the study area, tongues of freshwater that have moved south across the fault are still present.

Cross section A-A' (Figs 4.8, 4.10) is a west-east trending cross section. Areas of relatively freshwater (0-1 g/L) have moved south across the fault at intermediate depths and another area of relatively freshwater on the eastern side of the cross section at shallow depths crossed the fault from the north. On the eastern edge of the section, a relatively salty plume (20-100 g/L) is present between 1,000 and 2,500 feet (300 and 760 m). This plume of saline water is possibly from St. Gabriel, but may also be influenced by other salt structures outside of the study area. At depths greater than 3,000 feet (915 m) very high salinities are present (as high as 220 g/L). This deep saline water is present at depth over large areas of south Louisiana, and is from dissolution of salt (Hanor and Sassen, 1990).

Cross section B-B' (Figs 4.8, 4.11) shows large areas containing waters in the middle of the salinity range (1-10 g/L). A large area of high salinity (20-200 g/L) occurs at depths of 2,000 to 4,000 ft (600 to 1,200 m) on the western edge of the cross section, near the vicinity of the Bayou Choctaw dome. This dome may be responsible for the observed salinity highs, possibly

with input from other salt structures nearby. Another relatively salty area (30-100 g/L) on the

eastern side of the cross section is probably water originating from the St. Gabriel field, and

possibly other salt structures. A small area of fresher waters (0.3-1 g/L) from the north is present

in the shallower section on the eastern edge of the cross section.

Cross section C-C' (Figs 4.8, 4.12) shows a salinity profile with three well-defined zones,

a relatively saline zone in the shallow section (20-100 g/L), a middle zone of low salinity (1-20

g/L), and a zone of high salinity (100-320 g/L) at depth. The shallow section between 500-1,500

feet (460-910 m) contains an area of relatively salty water, which is part of the previously

discussed high salinity plume from St. Gabriel extending north through the MRAA and into the

area south of the fault. The intermediate zone of 1,500-3,000 ft (460-910 m) is a mixture of

fresher, less dense waters that have moved southward across the fault and more dense saline

waters which have migrated from the south. The spatial variations in salinity are analogous to

those in a salt-wedge estuary. This is shown with red arrows in Figure 4.12. The high salinity

zone at a depth of 3,000-4,000 feet (910-1,220 m) is part of the previously mentioned regional

brine from dissolution of salt regionally in south Louisiana.

The cross section C-C' was also examined using *in situ* fluid densities (Figure 4.13). This

shows that the spatial variations in density follow the same general pattern seen in spatial

variations in salinity. However, the variations in fluid densities immediately south of the fault in

the intermediate zone are much less than the corresponding variations in salinity. This is because

the increase in temperature with depth is partially offsetting the increase in density caused by an

increase in salinity. It is possible that fluid flow immediately south of the fault in the

intermediate zone could by modeled as an isodensity fluid system. The presence of the extremely

high density waters at depths greater than 3,000 ft (910 m) suggest that moving these very dense

waters vertically up the Baton Rouge fault might require much more hydraulic work than moving lower density brackish waters laterally across the fault. This would support the hypothesis that the saline waters have been transported laterally across the fault, and the source is likely due to dissolution of local salt domes south of the fault.

CONCLUSIONS

The research performed in this study has confirmed the observation of Bray and Hanor (1990) that there are plumes of saline water which extend vertically above the top of salt at the St. Gabriel field, which occurs at depths exceeding 10,000 ft (3,050 m), to essentially the water table. Most of the areas of elevated salinity are also areas of elevated temperature gradient, suggesting the simultaneous upward transport of both saline water and heat. Hypothetical one-dimensional, steady-state heat and solute transport calculations indicate that modest vertical upward fluid velocities on the order of a few cm/y could broadly account for the observed variations in salinities and temperatures at St. Gabriel. However, it is possible that the plumes have been produced instead by the episodic expulsion of waters from the overpressured sediments at depth at St. Gabriel, as has been proposed for the origin of the salinity plume at the Welsh salt dome in southwest Louisiana (Bennett and Hanor, 1987), a process which has been numerically modeled by Williams and Ranganathan (1994). Thus, the plumes at St. Gabriel may be the transient remnants of earlier dewatering events. The exact pathways of fluid migration at St. Gabriel were not established as part of this research, but the field is complexly faulted (Fig. 2.2), and multiple conduits for fluid flow may exist.

Spatial variations in formation water salinity support the conclusion that there has been lateral migration of saline waters northward from the St. Gabriel field toward the Baton Rouge fault. There have been two distinctly different pathways, a shallow plume of saline water which has migrated from the field to the northwest in the lower part of the Mississippi River Alluvial Aquifer (MRAA), and a more diffuse brackish zone below this where there has been mixing of saline waters from St. Gabriel with fresh meteoric waters from the Baton Rouge aquifer sands to the north. The presence of dense saline waters at shallow depths would have capacity to induce

60

density-driven lateral fluid flow (e.g., Williams and Ranganathan, 1994). In addition to the broad zone of mixing which exists south of the fault, there are areas where well-defined tongues of fresh water have moved laterally across the fault to the south. The is also evidence for the contribution of saline waters from salt domes west of the Mississippi River, which may include the Bayou Choctaw and/or White Castle salt domes (Welch and Hanor, 2011). Both the fresh waters north of the Baton Rouge fault and the brackish waters to the south overlie much more saline waters (as high as 320 g/L) at a depth of 3,000 feet (915 m) which represent the regional amalgamation of plumes of brine formed by the subsurface dissolution of the several salt domes south of Baton Rouge (Bray and Hanor, 1990). The results of the present research support the conclusion that there has been extensive lateral migration of waters across the Baton Rouge fault in the past rather than vertical migration up the fault. Although the presumed anisotropy in permeability of the fault zone should favor flow vertically up the fault over flow perpendicular to the fault, the large density contrast between the fresh and brackish waters above 3,000 feet (915 m) with the highly saline waters below may inhibit this.

An examination of the 3-D seismic data set which exists for the St. Gabriel field (Thomas Buerkhart, personal communication, 2012) could shed light on the pathways of fluid migration at the field. A planned regional study utilizing the results of this and of previous studies (Bray and Hanor,1990; Welch and Hanor, 2011; Wendeborn and Hanor, 2008) (Hanor, personal communication) should provide further insight into the role of salt dissolution on the regional and local hydrogeology of southeastern Louisiana.

REFERENCES

Bateman, R.M. and Konen, C.E. (1977) Wellsite log analysis and the programmable pocket
    calculator. Society Professional Well Log Analysts Transactions, vol. 18, pg B1-B35.

Bennett, S.S, and Hanor, J.S. (1987) Dynamics of subsurface salt dissolution at the Welsh dome,
    Louisiana gulf coast. Dynamical geology of salt and related structures, Academic Press
    Inc., pg 653-677.

Bense, V.F. and Person, M.A. (2006) Faults as conduit-barrier systems to fluid flow in siliclastic
    sedimentary aquifers. Water Resources Research, vol 42, wo5421.

Bray, R.B. and Hanor, J.S. (1990) Spatial variations in subsurface pore fluid properties in a
    portion of southeast Louisiana: Implications for regional fluid flow solute transport.
    Transactions- Gulf Coast Association of Geological Societies, vol. 40, pg 53-64.

Bredehoft, J.D. and Papadopulos, I.S. (1965) Rates of vertical groundwater movement estimated
    from the Earth's thermal profile. Water Resources Research, vol 1.2, pg 325-328.

Carlson, D. (2008) Anatomy of saltwater fronts observed within geophysical logs in East Baton
    Rouge Parish. Baton Rouge Geological Society, Second Annual Louisiana Groundwater
    Program, Abstracts, pg 13.

Finlayson, B.A. (1992) Numerical methods for problems with moving fronts. Seattle: Ravenna
    Park Publishing.

Gearhart-Owen Wireline Services. (1974) Formation Evaluation Data Handbook. Gearhart-
    Owen Industries Inc, U.S.A.

Griffith, J.M. (2003) Hydrogeologic framework of southeastern Louisiana: Louisiana
    Department of Transportation and Development. Water Resources Technical Report no.
    72, pg 21.

Hanor, J.S. (1984) Salinity and geochemistry of subsurface brines in South Louisiana and their
    potential for reaction with injected geothermal waste waters. United States Department of
    Energy Report DOE/NV/10174-3.

Hanor, J.S., Bray, R.B., and Nunn, J.A. (2007) Why are the principal discharge areas of the
    coastal lowlands aquifer system in Louisiana located as much as 100 km from the coast?,
    First Annual Louisiana Groundwater Symposium; Louisiana Geological Survey, Baton
    Rouge, pg. 69 – 72.

Hanor, J.S. and Mercer, J.A. (2010) Spatial variations in the salinity of pore waters in northern
    deep water Gulf of Mexico sediments: implications for pathways and mechanisms of
    solute transport. Geofluids, vol 10 (1-2), pg 83-93.

Hanor, J.S. and Sassen, R. (1990) Evidence for large scale vertical and lateral migration of formation waters, dissolved salt, and crude oil in the Louisiana gulf coast. GCSSEMP Foundation ninth annual research conference, pg 283-296.

Holyoak, D.M. (1965) St. Gabriel field: Ascension and Iberville Parishes, Louisiana. New Orleans Geological Society (NOGS), pg.146-149.

Long, R.A. (1965) Groundwater in the Geismar-Gonzales area, Ascension Parish, Louisiana. Water Resources Bulletin, No. 7.

Lovelace, J.K. (2007) Chloride concentrations in ground water in East and West Baton Rouge Parishes, Louisiana, 2004-05. Scientific Investigations Report 2007-5069.

Martin, A. and Whiteman, C.D. (1989) Geohydrology and regional ground-water flow of the coastal lowlands aquifer system in pats of Louisiana, Mississippi, Alabama, and Florida-a preliminary analysis: USGS Water Resources Investigations Report 88-4100, 88 p.

McCulloh, R.P. and P.V. Heinrich (2012) Surface Faults of the South Louisiana Growth-Fault Province, in Cox, R.T., M. Tuttle, O. Boyd, and J. Locat, eds., Recent Advances in North American Paleoseismology and Neotectonics east of the Rockies and Use of the Data in Risk Assessment and Policy, Geological Society of America (in review).

McFarlan, E, Jr. and LeRoy, D.O. (1988) Subsurface geology of the late Tertiary and Quaternary deposits, coastal Louisiana and the adjacent continental shelf. Transactions- Gulf Coast Association of Geological Societies, vol 38, pg 421-433.

Phillips, S. L., H. Ozbeck, and L. F. Silvester (1983), Density of sodium chloride solutions at high temperatures and pressures. Rep. LBL-16275, 51 pp., Lawrence Berkeley Natl. Lab., Berkeley, Calif.

Roberts, S.J. and Nunn, J.A. (1995) Episodic fluid expulsion from geopressured sediments. Marine and Petroleum Geology, vol 12. pg 195-204.

Rollo, J.R. (1969) Saltwater encroachment in aquifers of the Baton Rouge area, Louisiana. Water Resources Bulletin, No. 13.

Salvador, A. (1991) Origin and development of the Gulf of Mexico basin: in, Salvador, A., ed., The Gulf of Mexico Basin: The Geology of North America, Volume J, pg 389-444.

Stoessell, R.K. and Prochaska, L. (2005) Chemical evidence for migration of deep formation fluids into shallow aquifers in south Louisiana. Gulf Coast Association of Geological Societies Transactions, vol 55, pg 294-309.

Stuyfzand, P.J. (1991) Composition genesis and quality variations of shallow groundwater in coastal dunes. (in Dutch). KIWA SWE-91.008, pg 175.

Tsai, F.T-C. (2010) Bayesian model averaging assessment on groundwater management under model structure uncertainty. Stochastic Environmental Research and Risk Assessment, vol 24, pg 845-861.

Tsai, F.T-C. and Li, X. (2008) Saltwater intrusion and hydraulic conductivity estimation in East Baton Rouge Parish, Louisiana. 20th Salt Water Intrusion Meeting.

Welch, S.E. and Hanor, J.S. (2011) Sources of elevated salinity in the Mississippi River Alluvial Aquifer, south-central Louisiana, USA. Applied Geochemistry, 26, pg 1446-1451.

Wendeborn, F.C. and Hanor, J.S. (2008) Controls of major solute composition of groundwater in the eastern portion of the Southern Hills regional aquifer system, Mississippi and Louisiana.

Wendeborn, F.C. and Hanor, J.S. (2009) The Baton Rouge fault, south Louisiana: a barrier and/or conduit for vertical and/or lateral groundwater flow? Baton Rouge Geological Society: 3rd Annual Louisiana Groundwater and Water Resource Symposium [abstract]

Whiteman, C.D. (1972). Groundwater in the Plaquemine-White Castle area Iberville Parish, Louisiana. Water Resources Bulletin No. 16.

Williams, M.D. and Ranganathan, V. (1994) Ephemeral thermal and solute plumes formed by upwelling groundwaters near salt domes, Journal of Geophysical Research, vol 99, No. B8, pg 15,667-15,681.

APPENDIX I: BOREHOLE LOG INFORMATION

Abbreviations:

LGS: Louisiana Geological Society

BHF: Braden Head Flange

GL: Ground Level

Well or Borehole Name	Designation used in this study	Field Area	UTM coodinates	SONRIS number	USGS number	Date of last logging run	Log Datum	Source of log
FB Gueymard #1	LGS1	St. Gabriel	15N 685996 3348899	33267		7/19/1947	1-ft above rotary	LGS
HH Gueymard #2	LGS2	St. Gabriel	15N 688077 3349911	26004		6/6/1941	1-ft above rotary	LGS
HH Gueymard #3	LGS3	St. Gabriel	15N 687903 3349952	26109		7/21/1941	1-ft above rotary	LGS
Gueymard #4	LGS4	St. Gabriel	15N 688045 3350076	26409		8/20/1941	1-ft above rotary	LGS
Gueymard #6	LGS5	St. Gabriel	15N 688042 3349710	26592		11/21/1941	1-ft above rotary	LGS
HH Gueymard #10	LGS6	St. Gabriel	15N 686658 3350097	33189		8/8/1947	1-ft above rotary	LGS
Gueymard #B-2	LGS7	St. Gabriel	15N 688239 3349980	26289		8/16/1941	1-ft above rotary	LGS
Gueymard #B-3	LGS8	St. Gabriel	15N 688243 3349736	26497		10/2/1941	1-ft above rotary	LGS
Gueymard #B-4	LGS9	St. Gabriel	15N 688246 3349548	26738		9/7/1941	1-ft above rotary	LGS
Gueymard #B-5	LGS10	St. Gabriel	15N 688468 3349552	26835		2/11/1942	1-ft above rotary	LGS
Harry B Nelson #1	LGS11	St. Gabriel	15N 679766 3344349	38939		10/29/1949	1-ft above rotary	LGS
Louis Carville #1	LGS12	St. Gabriel	15N 686422 3346456	67742		11/15/1957	1-ft above rotary	LGS
Natalbany Lbr. Co. #A-1	LGS13	St. Gabriel	15N 685928 3350062	28638		11/6/1943	1-ft above rotary	LGS
Natalbany #B-3	LGS14	St. Gabriel	15N 687621 3350091	25946		6/19/1941	1-ft above rotary	LGS
Natalbany #J-1	LGS15	St. Gabriel	15N 686287 3350468	28413		7/8/1943	drive bushing	LGS
Opdenweyer-Alcus Cypress Co. #1	LGS16	St. Gabriel	15N 686684 3351994	72319		5/21/1959	1-ft above rotary	LGS
SG Nelson et al. #1	LGS17	St. Gabriel	15N 679500 3342959	74105		4/17/1959	1-ft above rotary	LGS
Union Texas Petroleum Corp. No. 1	LGS18	St. Gabriel	15N 687647 3348090	190387		3/17/1984	BHF	LGS
Natalbany #1	LGS19	St. Gabriel	15N 687037 3348219	31356		2/18/1946	1-ft above rotary	LGS
Gueymard #1	LGS20	St. Gabriel	15N 687833 3350106	25755		4/19/1941	1-ft above rotary	LGS
State Prison Farm #1	LGS21	St. Gabriel	15N 685381 3349355	43785		5/17/1941	1-ft above rotary	LGS
Opdenweyer-Alcus Cypress Company No.3	2	St. Gabriel	N15 685979 3351883			10/28/1968	BHF	Hanor
Opdenweyer-Alcus Cypress No.5	3	St. Gabriel	N15 685794 3352280			9/7/1969	1-ft above rotary	Hanor

Name	No.	Parish	Coordinates			Date		Source
Opdenweyer-Alcus Cypress No.6	4	St. Gabriel	N15 686170 3352502			3/29/1970	BHF	Hanor
J.B. LeBlanc et al. No. 1	5	St. Gabriel	N15 685506 3351854			2/4/1969	1-ft above rotary	Hanor
J.B. LeBlanc et al. No.2	6	St. Gabriel	N15 685372 3352267			10/4/1969	BHF	Hanor
Opdenweyer-Alcus Cypress No.1	7	St. Gabriel	N15 686579 3352204			1/2/1973	GL	Hanor
Opdenweyer-Alcus Cypress #1	8	St. Gabriel	N15 686803 3351817			5/21/1959		Hanor
Opdenweyer-Alcus Cypress No.1	9	St. Gabriel	N15 686551 3352779			3/2/1981	BHF	Hanor
Opdenweyer-Alcus Cypress No.1	11	St. Gabriel	N15 686345 3351184			6/11/1967	BHF	Hanor
J.H. Hauberg et al No. 1	13	St. Gabriel	N15 685752 3350844			2/12/1971	BHF	Hanor
J.H. Hauberg #1	14	St. Gabriel	N15 686208 3350527			2/23/1978	BHF	Hanor
John H. Hauberg No. 1	15	St. Gabriel	N15 686528 3350809			3/9/1969	BHF	Hanor
Natalbany Lumber Company No. 1	17	St. Gabriel	N15 686815 3350430			7/7/1961	1-ft above rotary	Hanor
Natalbany Lumber Company A-1	18	St. Gabriel	N15 685938 3349944			11/6/1943	1-ft above rotary	Hanor
H.H. Gueymard No. 16	19	St. Gabriel	N15 686501 3349878			10/31/1979	BHF	Hanor
F.B. Gueymard #1	20	St. Gabriel	N15 686058 3348876			7/21/1947	1-ft above rotary	Hanor
Carville #1 composite	21	St. Gabriel	N15 686712 3347463			7/1/1949	1-ft above rotary	Hanor
Louis Carville #1	22	St. Gabriel	N15 686657 3346227			11/15/1957	1-ft above rotary	Hanor
Opdenweyer-Alcus Cypress #A-1	23	St. Gabriel	N15 687644 3352729			9/29/1951	1-ft above rotary	Hanor
Opdenweyer-Alcus Cypress No.2	24	St. Gabriel	N15 687307 3352220			7/29/1973	GL	Hanor
Opdenweyer-Alcus Cypress Co. No. 2	25	St. Gabriel	N15 687550 3351882			10/13/1976	BHF	Hanor
LeBlanc-State No. 1	26	St. Gabriel	N15 688483 3352072			2/11/1978	BHF	Hanor
Opdenweyer-Alcus Cypress Company No.1	28	St. Gabriel	N15 687573 3351178			10/25/1948	BHF	Hanor
Mary Walker Goston #1	29	St. Gabriel	N15 687592 3350840			6/20/1948	1-ft above rotary	Hanor
Gueymard #A-2	30	St. Gabriel	N15 687180 3350476			5/25/1954	1-ft above rotary	Hanor
Natalbany #A-5	32	St. Gabriel	N15 688392 3350573			7/7/1947	1-ft above rotary	Hanor
C. Fourroux et al. No. 1	34	St. Gabriel	N15 687094 3349433			9/25/1966	1-ft above rotary	Hanor
Richard #1	35	St. Gabriel	N15 687120 3348969			4/19/1976	BHF	Hanor
Natalbany Well No. 1	37	St. Gabriel	N15 687863 3349028			7/3/1974	BHF	Hanor
Natalbany #1	38	St. Gabriel	N15 687660 3349028			1/18/1939		Hanor

Exploration-Natalbany Lbr #1	39	St. Gabriel	N15 688139 3349207			1/29/1967	BHF	Hanor
Natalbany #1	41	St. Gabriel	N15 687198 3348078			2/16/1946	1-ft above rotary	Hanor
Caldwell #2	42	St. Gabriel	N15 687913 3347419			2/18/1947	1-ft above rotary	Hanor
Natalbany Lumber Company # 1	44	St. Gabriel	N15 689021 3351352			12/19/1959	1-ft above rotary	Hanor
Natalbany #1	45	St. Gabriel	N15 689205 3350859			1/6/1944	1-ft above rotary	Hanor
Natalbany Lumber Company # 2	46	St. Gabriel	N15 690082 3351631			12/29/1960	1-ft above rotary	Hanor
F.W. Reimers #1	47	St. Gabriel	N15 689628 3351054			7/30/1979		Hanor
John H. Hauberg No. 1	48	St. Gabriel	N15 689371 3350422			5/22/1969	BHF	Hanor
Allied Chemical #1	51	St. Gabriel	N15 689311 3348480			10/1/1979	BHF	Hanor
W.E. Caldwell #1	52	St. Gabriel	N15 688594 3348250			3/17/1955	1-ft above rotary	Hanor
W.E. Caldwell #1	53	St. Gabriel	N15 689335 3347704			3/28/1952	1-ft above rotary	Hanor
Riverside Plantation #1	54	St. Gabriel	N15 689037 3346201			5/20/1960	1-ft above rotary	Hanor
Unit 5 Well #1	55	St. Gabriel	N15 687171 3351204			9/9/1953	1-ft above rotary	Hanor
Natalbany #8	56	St. Gabriel	N15 687674 3349480			3/27/1951	1-ft above rotary	Hanor
Opdenweyer-Alcus Cypress Co. No. 2	60	St. Gabriel	N15 685940 3351588			7/19/1968	BHF	Hanor
Opdenweyer-Alcus Cypress Company #4	61	St. Gabriel	N15 686353 3351490			12/17/1968	1-ft above rotary	Hanor
Natalbany #J-1	62	St. Gabriel	N15 686290 3350450			7/8/1943	drive bushing	Hanor
Natalbany #J-2	63	St. Gabriel	N15 686281 3350787			log unclear		Hanor
Gueymard No. 9	64	St. Gabriel	N15 686359 3349993			7/12/1944	1-ft above rotary	Hanor
H.H. Gueymard No. 10	65	St. Gabriel	N15 686737 3350018			6/30/1947	1-ft above rotary	Hanor
Cypress Well #2	67	St. Gabriel	N15 687630 3351538			10/14/1949	1-ft above rotary	Hanor
Ponchartrain 1E	69	St. Gabriel	N15 688377 3351165			9/3/1950	1-ft above rotary	Hanor
Gueymard #A-1	70	St. Gabriel	N15 687657 3350443			4/2/1941	1-ft above rotary	Hanor
Natalbany #A-8	71	St. Gabriel	N15 687992 3350851			12/19/1949	1-ft above rotary	Hanor
H.H. Gueymard #1	75	St. Gabriel	N15 687206 3349730			11/22/1959	1-ft above rotary	Hanor
H.H. Gueymard #2	76	St. Gabriel	N15 687255 3349768			4/7/1960	1-ft above rotary	Hanor
Gueymard #B-1	77	St. Gabriel	N15 687475 3350149			7/12/1941	1-ft above rotary	Hanor

Gueymard #B-2	78	St. Gabriel	N15 687718 3349936			4/16/1941	1-ft above rotary	Hanor
Natalbany #B-3	79	St. Gabriel	N15 687712 3350139			6/19/1941	1-ft above rotary	Hanor
Gueymard #1	82	St. Gabriel	N15 687944 3350136			4/19/1941	1-ft above rotary	Hanor
Gueymard #4	83	St. Gabriel	N15 688115 3350097			8/20/1941	1-ft above rotary	Hanor
Gueymard #5	84	St. Gabriel	N15 687916 3349752			11/12/1941	1-ft above rotary	Hanor
H.H. Gueymard #2	85	St. Gabriel	N15 688108 3349957			6/7/1941	1-ft above rotary	Hanor
Gueymard #6	87	St. Gabriel	N15 688111 3349796			11/21/1941	1-ft above rotary	Hanor
Gueymard #7	88	St. Gabriel	N15 687928 3349561			10/18/1941	1-ft above rotary	Hanor
Gueymard #8	89	St. Gabriel	N15 688122 3349532			12/13/1941	1-ft above rotary	Hanor
Gueymard Well No. 1	90	St. Gabriel	N15 688322 3350087			5/17/1974	BHF	Hanor
Gueymard No. 2	91	St. Gabriel	N15 688304 3349938			3/18/1978	BHF	Hanor
Mrs. F.B. Gueymard No.1	94	St. Gabriel	N15 688813 3349210			8/2/1949	1-ft above rotary	Hanor
Water well #3	A1	Cinclare Central Factory	N15 669631 3364084		121-23	8/9/1946	1-ft above rotary	Tsai
Brusly Water District	A2	Brusly	N15 670122 3365108		121-53	6/26/1958	1-ft above rotary	Tsai
Perkins Road #1	A5	Water Well	N15 682127 3364009		033-703	7/21/1959	1-ft above rotary	Tsai
Siegen Lane	A6	BR Water Works	N15 686090 3363337		033-638	7/17/1957	at rotary	Tsai
U.S. Geological Survey No. EB 803	A7	Water Well	N15 688257 3363097		033-803	2/7/1966	GL	Tsai
Elliot Road well #1	A8	Water Well	N15 693400 3360723		033-1156	10/31/1974	GL	Tsai
Mallard Lake #2	A13		N15 698628 3359647		033-1319	11/12/2002	GL	Tsai
DOW Chemical Co. Test Hole #6	B4	Water Well	N15 669185 3356686		121-140	11/12/1974	GL	Tsai
LWRRI 67-6	B8	Water Well	N15 679531 3357930		033-826	5/19/1967	GL	Tsai
EB 931	B10		N15 689215 3358709		033-931	5/15/1974	GL	Tsai
Jayces Fairground well #EB-932	B11	Water Well	N15 692335 3359041		033-932	5/23/1974	GL	Tsai
LSU #1	A3	Wildcat	N15 674865 3361155	65240		5/27/1957	1-ft above rotary	Tsai
Russell Kleinpeter #1	A4	W.C. Bayou Fountain	N15 677806 3361203	83393		5/28/1961	1-ft above rotary	Tsai
S.P. Schwing #1	B1	W. Addis	N15 658423 3360693	68545		12/14/1957	1-ft above rotary	Tsai

Wilbert et al. and son #1	B2	N. Bayou Choctaw	N15 662211 3357456	73788		5/11/1959	1-ft above rotary	Tsai
Levert Heirs #C-1	B3	Bayou Choctaw	N15 663531 3356001	69635		4/24/1958	1-ft above rotary	Tsai
Australia Planting Co. #1	B6	Wildcat	N15 67437 3358364	49205		9/15/1953	1-ft above rotary	Tsai
Anstralia Planting Co. #1	B7	Wildcat	N15 676008 3357681	63144		11/21/1956	1-ft above rotary	Tsai
V.J. Gianelloni #2	B9	Burtville	N15 683621 3356764	41855		2/6/1951	1-ft above rotary	Tsai

APPENDIX II: SENSITIVITY STUDY OF VERTICAL TRANSPORT EQUATIONS

Values used for Bredehoft and Papadopulos (1965) equation:

Symbol	Name	Value Used in Study	units
z(U)	depth, upper	0	m
z(L)	depth, lower	6,000	m
T(z)	temperature at intermediate depth		K
T(U)	temperature at upper boundary	25	K
T(L)	temperature at lower boundary	160	K
β	a dimensionless parameter		
c_w	specific heat capacity	4181.3	J/(kg*K)
ρ_w	density	1,000	kg/m^3
q_w	Darcy velocity	3.00E-10	m/s
L	distance between constant temperature boundaries	6,000	m
K_m	Thermal conductivity of porous medium	2	J/(m*s*K)

Values used for Finlayson (1992) equation:

Symbol	Name	Value Used in Study	Units
z(U)	depth, upper	0	m
z(L)	depth, lower	6,000	m
C(z)	concentration at intermediate depth		kg/L
C(U)	concentration at upper boundary	0	kg/L
C(L)	concentration at lower boundary	190	kg/L
ξ	a dimensionless parameter		
Φ	porosity	0.4	m^3/m^3
αL	longitudinal dispersivity	100	m
q_w	Darcy velocity	3.00E-10	m/s
L	distance between constant temperature boundaries	6,000	m
D_m	sediment diffusion coefficient	1.00E-09	m^2/s

The values used in this study were chosen as a best match to data from the St. Gabriel field, but the equations were also studied for sensitivity with changes of Darcy velocity. The best match to the St. Gabriel dataset is a Darcy velocity of 5.5E-10 m/s, or a true velocity of 2.4 cm/y.
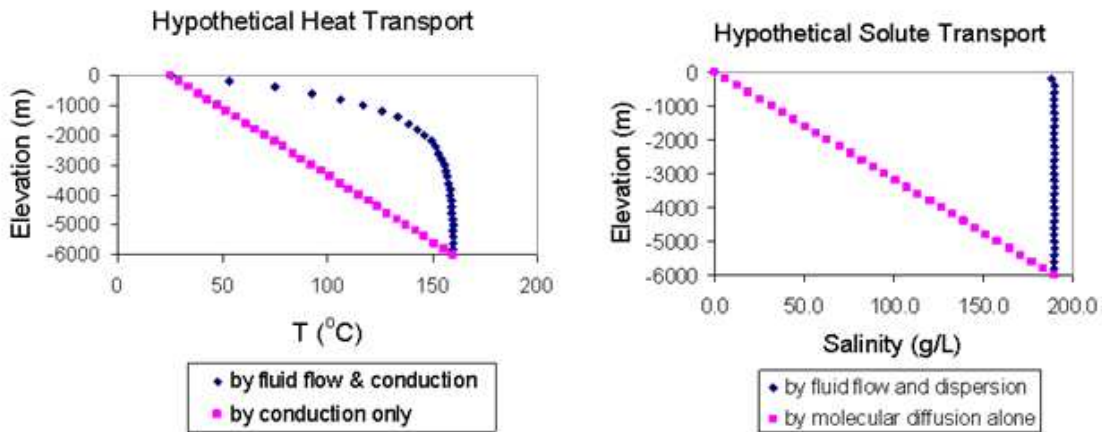
With an increase of the Darcy velocity by a factor of 2, changes in the vertical transport of heat and solute can be investigated. Using a Darcy velocity of 1E-9 m/s, with a true velocity of 7.8 cm/y.
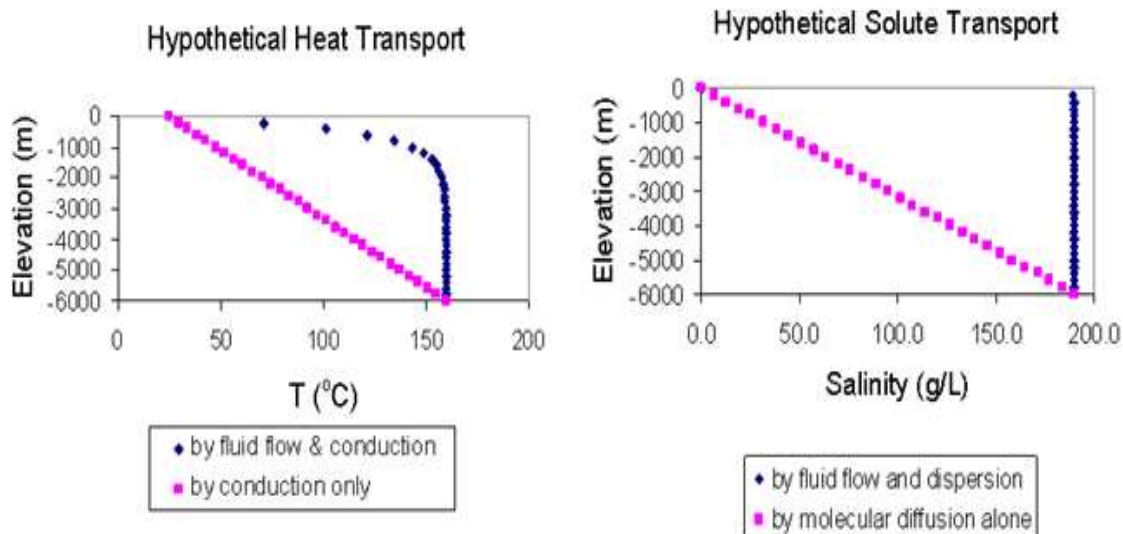
This increase in Darcy's velocity shows a change in the affects of vertical transport with fluid flow and conduction. Higher temperatures can be found at shallower depths before the temperature begins to decrease. No significant changes are noticed in the solute transport model, suggesting that temperature is more sensitive to increases in Darcy's velocity than salinity.

With a decrease of the Darcy velocity by a factor of 2, changes in the vertical transport of heat and solute can be investigated. A Darcy velocity of 2.75E-10 m/s, a true velocity of 2.16 cm/y was used.

Hypothetical Heat Transport

- ◆ by fluid flow & conduction
- ■ by conduction only

Hypothetical Solute Transport

- ◆ by fluid flow and dispersion
- ■ by molecular diffusion alone
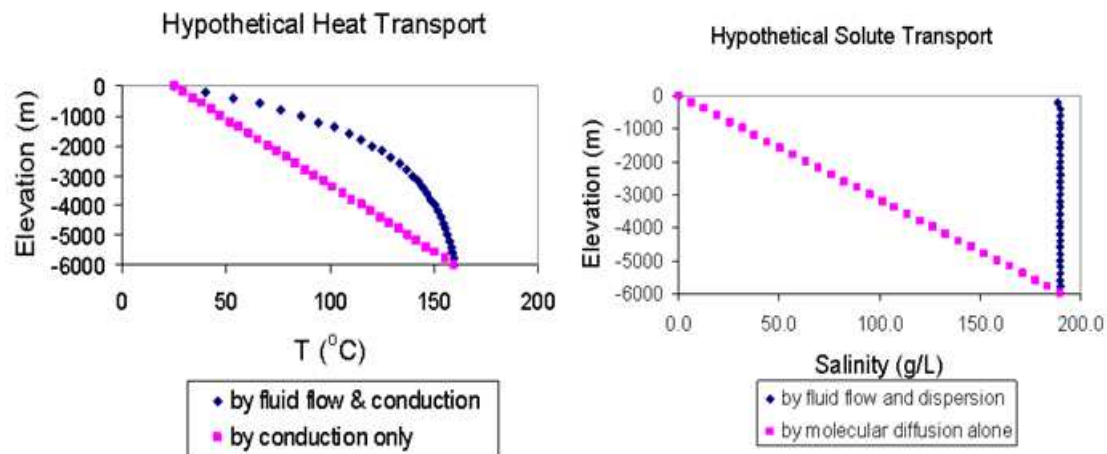
This decrease in the Darcy velocity causes high temperatures to lessen in deeper areas, shifting closer to the line showing transport by conduction only. Again, the solute transport model shows no significant change, suggesting that, like seen with an increase in Darcy velocity, heat transport is more sensitive to decreases in Darcy's velocity.

VITA

Callie Elizabeth Anderson was born in 1988, in Kenner, Louisiana. She graduated from Destrehan High School in May 2006. In August of 2006, she enrolled at Louisiana State University as a General Studies major. After taking several geology classes, she discovered a love of earth science and graduated with a Bachelor Degree of Science in geology in May 2010. In August of 2010, Callie returned to Louisiana State University in the Graduate Program to study the saltwater intrusion of the Baton Rouge aquifer system under Dr. Jeffrey Hanor. Callie will graduate with a Master of Science in geology and geophysics in May 2012.